Supplementary material

The WoKaS-Iso Database: Workflow for a Global Compilation of Oxygen-18 and Deuterium Records in Karst Springs and Cave Drip Water for Enhanced Understanding of Karst Systems

Yining Zang[1]*, Pauline C.Treble[2,3]*, Kei Yoshimura[4,5], Jayson Gabriel Pinza[6,7], Fengbo Zhang[8], Kübra Özdemir Çallı[1], Xiaojun Mei[9], Admin Husic[10], Alena Gessert[11], Andrej Stroj[12], Bartolomé Andreo[13], Bernard Ladouche[14,15,], Christine Stumpp[16], Diana Mance[17], Eleni Zagana[18], Fen Huang[19], Giuseppe Sappa[20], Harald Kunstmann[21,22], Heike Brielmann[23], Hong Zhou[24], Huaying Wu[19], Jakob Garvelmann[21,25], James Berglund[26], Jean-Baptiste Charlier[14,15], Jens Lange[27], Juan Antonio Barberá Fornell[13], Junbing Pu[28], Konstantina Katsanou[29], Kun Ren[19], Laura Toran[30], Laurence Gill[31], Maria Filippini[32], Martin Kralik[33], Matías Mudarra Martínez[13], Min Zhao[34], Mingming Luo[24], Nico Goldscheider[35], Nikolaos Lambrakis[18], Pantaleone De Vita[36], Qiong Xiao[19], Shi Yu[19], Silvia Iacurto[20], Silvio Coda[36], Ted McCormack[37], Vincenzo Allocca[36], W. George Darling[38], Walter D'Alessandro[39], Xulei Guo[24], Yundi Hu[40], Zhijun Wang[41], Eva Kaminsky[42,43], Jiří Faimon[44,45], Marek Lang[44], Pavel Pracný[44], Andreas Hartmann[1]

* Corresponding authors

[1]Institute of Groundwater Management, Technical University of Dresden, Dresden, 01069, Germany
[2]ANSTO, New Illawarra Road, Lucas Heights, NSW 2234, Australia
[3]School of Biological, Earth and Environmental Sciences, UNSW Sydney, Sydney NSW, 2052, Australia
[4]Institute of Industrial Science, The University of Tokyo, Kashiwa, Japan
[5]Japan Atmosphere and Ocean Research Institute, The University of Tokyo, Kashiwa, Japan
[6]ECOSPHERE Research Group, University of Antwerp, Universiteitsplein 1C, 2610 Antwerp, Belgium
[7]Division of Soil and Water Management, KU Leuven, Celestijnenlaan 200E, 3001 Leuven, Belgium
[8]Ningbo River Management Center, Ningbo Water Resources Bureau, Ningbo 315000, China
[9]Merchant Marine College, Shanghai Maritime University, Shanghai 201306, China
[10]Department of Civil and Environmental Engineering, Virginia Tech, Blacksburg 24061, USA
[11]Institute of Geography, Faculty of Sciences, University of P.J. Šafárik, 040 01 Košice, Slovakia
[12]Croatian Geological Survey, Sachsova 2, 10000 Zagreb, Croatia
[13] Department of Geology and Centre of Hydrogeology at the University of Malaga, 29071, Malaga, Spain
[14]BRGM, Univ Montpellier, Montpellier, France
[15]G-EAU, Univ Montpellier, AgroParisTech, BRGM, CIRAD, INRAE, Institut Agro, IRD, Montpellier, France
[16]Institute of Soil Physics and Rural Water Management, Department of Landscape, Water and Infrastructure, BOKU University, Vienna, Austria
[17]Faculty of Physics, University of Rijeka, 51000, Rijeka, Croatia
[18]Laboratory of Hydrogeology, Department of Geology, Faculty of Natural Sciences, University of Patras, GR-26504 Patras, Greece
[19]Key Laboratory of Karst Dynamics, MNR and GZAR, Institute of Karst Geology, Chinese Academy of Geological Sciences, Guilin, 541004, China

[20]Department of Civil, Constructional and Environmental Engineering (DICEA), Sapienza University of Rome, 00184 Rome, Italy
[21]Institute of Meteorology and Climate Research, Karlsruhe Institute of Technology, Campus Alpin, D-82467 Garmisch-Partenkirchen, Germany
[22]Institute of Geography, University of Augsburg, D-86135 Augsburg, Germany
[23]Environment Agency Austria, Groundwater Unit, Spittelauer Laende 5, A-1090 Vienna, Austria
[24]School of Environmental Studies& Institute of Geological Survey, China University of Geosciences, Wuhan, 430074, Hubei, China
[25]Boden & grundwasser Allgäu GmbH, D-87527 Sonthofen, Germany
[26]Department of Civil and Environmental Engineering, University of Wisconsin – Platteville, Platteville, Wisconsin, USA
[27]Hydrology, University of Freiburg, 79098 Freiburg, Germany
[28]Chongqing Key Laboratory of Carbon Cycle and Carbon Regulation of Mountain Ecosystem, School of Geography and Tourism, Chongqing Normal University, Chongqing, 401331, China
[29]Department of Water Resources and Ecosystems, IHE Delft Institute for Water Education, Delft, Netherlands
[30]Department of Earth and Environmental Science, Temple University, Philadelphia, Pennsylvania, USA
[31]Department of Civil, Structural and Environmental Engineering, Trinity College Dublin, Ireland
[32]Department of Biological, Geological and Environmental Sciences—BiGeA, Alma Mater Studiorum, University of Bologna, Via Selmi 3, 40126 Bologna, Italy
[33]Department of Environmental Geosciences, Center for Microbiology and Environmental Systems Science, University of Vienna, 1090 Vienna, Austria
[34]State Key Laboratory of Environmental Geochemistry (SKLEG), Institute of Geochemistry, Chinese Academy of Sciences (CAS), Guiyang, China
[35]Institute of Applied Geosciences, Karlsruhe Institute of Technology, D-76131 Karlsruhe, Germany
[36]Department of Earth, Environmental and Resources Sciences (DiSTAR), University of Naples Federico II, Naples, Italy
[37]Geological Survey Ireland, Booterstown Avenue, Booterstown, Blackrock, Ireland
[38]British Geological Survey, Wallingford OX10 8BB, United Kingdom
[39]Istituto Nazionale di Geofisica e Vulcanologia – Sezione di Palermo, Via La Malfa 153, 90146 Palermo, Italy
[40]School of Geography and Environmental Science, Guizhou Normal University, Guiyang 550001, People's Republic of China
[41]Faculty of Arts and Sciences, Beijing Normal University, Zhuhai 519087, China
[42]Karst and Cave Group, Geological Paleontological Department, Natural History Museum, Vienna, Austria
[43]Institute of Soil Physics and Rural Water Management, Department of Landscape, Water and Infrastructure, BOKU University, Vienna, Austria
[44]Department of Geological Sciences, Faculty of Science, Masaryk University, Brno, Czech Republic
[45]Czech Geological Survey, Brno Branch, Brno, Czech Republic

Correspondence to: Yining Zang (yining.zang@tu-dresden.de), Pauline C.Treble (ptr@ansto.gov.au)

S1 δ¹⁸O time series analysis

Figure S1 shows the time series comparison of modelled and observed monthly $\delta^{18}O$ in precipitation at the 51 sites. Observations (red stars) are compared with estimates from the Sine Curve model (dashed blue line), IsoGSM (purple crosses), and the Isoscape model (green circles). Each panel shows the number of monthly observations (n.obs) and model performance statistics (R^2 and RMSE).

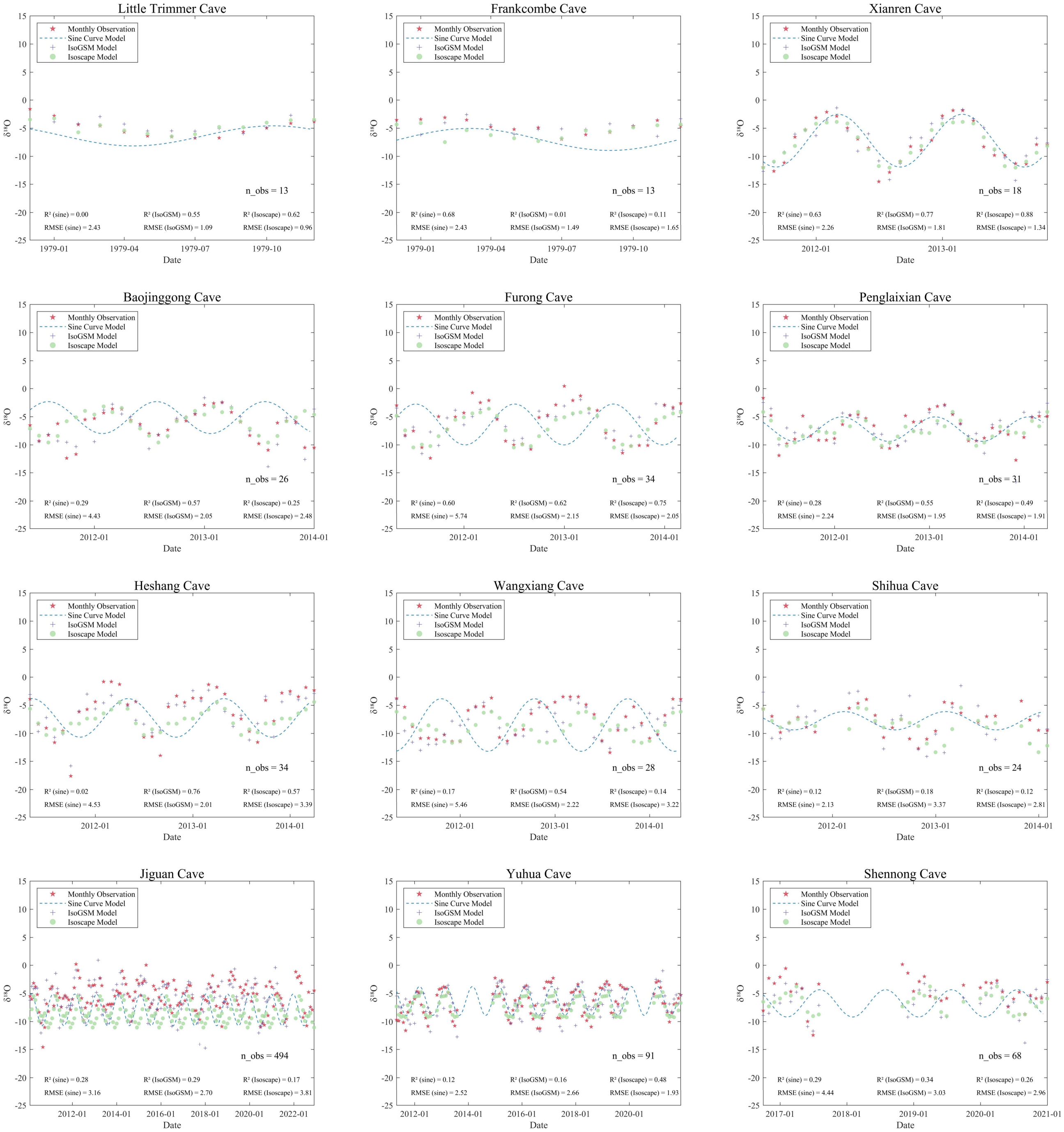
Little Trimmer Cave
n_obs = 13
R² (sine) = 0.00
R² (IsoGSM) = 0.55
R² (Isoscape) = 0.62
RMSE (sine) = 2.43
RMSE (IsoGSM) = 1.09
RMSE (Isoscape) = 0.96
Frankcombe Cave
n_obs = 13
R² (sine) = 0.68
R² (IsoGSM) = 0.01
R² (Isoscape) = 0.11
RMSE (sine) = 2.43
RMSE (IsoGSM) = 1.49
RMSE (Isoscape) = 1.65
Xianren Cave
n_obs = 18
R² (sine) = 0.63
R² (IsoGSM) = 0.77
R² (Isoscape) = 0.88
RMSE (sine) = 2.26
RMSE (IsoGSM) = 1.81
RMSE (Isoscape) = 1.34
Baojinggong Cave
n_obs = 26
R² (sine) = 0.29
R² (IsoGSM) = 0.57
R² (Isoscape) = 0.25
RMSE (sine) = 4.43
RMSE (IsoGSM) = 2.05
RMSE (Isoscape) = 2.48
Furong Cave
n_obs = 34
R² (sine) = 0.60
R² (IsoGSM) = 0.62
R² (Isoscape) = 0.75
RMSE (sine) = 5.74
RMSE (IsoGSM) = 2.15
RMSE (Isoscape) = 2.05
Penglaixian Cave
n_obs = 31
R² (sine) = 0.28
R² (IsoGSM) = 0.55
R² (Isoscape) = 0.49
RMSE (sine) = 2.24
RMSE (IsoGSM) = 1.95
RMSE (Isoscape) = 1.91
Heshang Cave
n_obs = 34
R² (sine) = 0.02
R² (IsoGSM) = 0.76
R² (Isoscape) = 0.57
RMSE (sine) = 4.53
RMSE (IsoGSM) = 2.01
RMSE (Isoscape) = 3.39
Wangxiang Cave
n_obs = 28
R² (sine) = 0.17
R² (IsoGSM) = 0.54
R² (Isoscape) = 0.14
RMSE (sine) = 5.46
RMSE (IsoGSM) = 2.22
RMSE (Isoscape) = 3.22
Shihua Cave
n_obs = 24
R² (sine) = 0.12
R² (IsoGSM) = 0.18
R² (Isoscape) = 0.12
RMSE (sine) = 2.13
RMSE (IsoGSM) = 3.37
RMSE (Isoscape) = 2.81
Jiguan Cave
n_obs = 494
R² (sine) = 0.28
R² (IsoGSM) = 0.29
R² (Isoscape) = 0.17
RMSE (sine) = 3.16
RMSE (IsoGSM) = 2.70
RMSE (Isoscape) = 3.81
Yuhua Cave
n_obs = 91
R² (sine) = 0.12
R² (IsoGSM) = 0.16
R² (Isoscape) = 0.48
RMSE (sine) = 2.52
RMSE (IsoGSM) = 2.66
RMSE (Isoscape) = 1.93
Shennong Cave
n_obs = 68
R² (sine) = 0.29
R² (IsoGSM) = 0.34
R² (Isoscape) = 0.26
RMSE (sine) = 4.44
RMSE (IsoGSM) = 3.03
RMSE (Isoscape) = 2.96
Monthly Observation
Sine Curve Model
IsoGSM Model
Isoscape Model
δ¹⁸O
Date

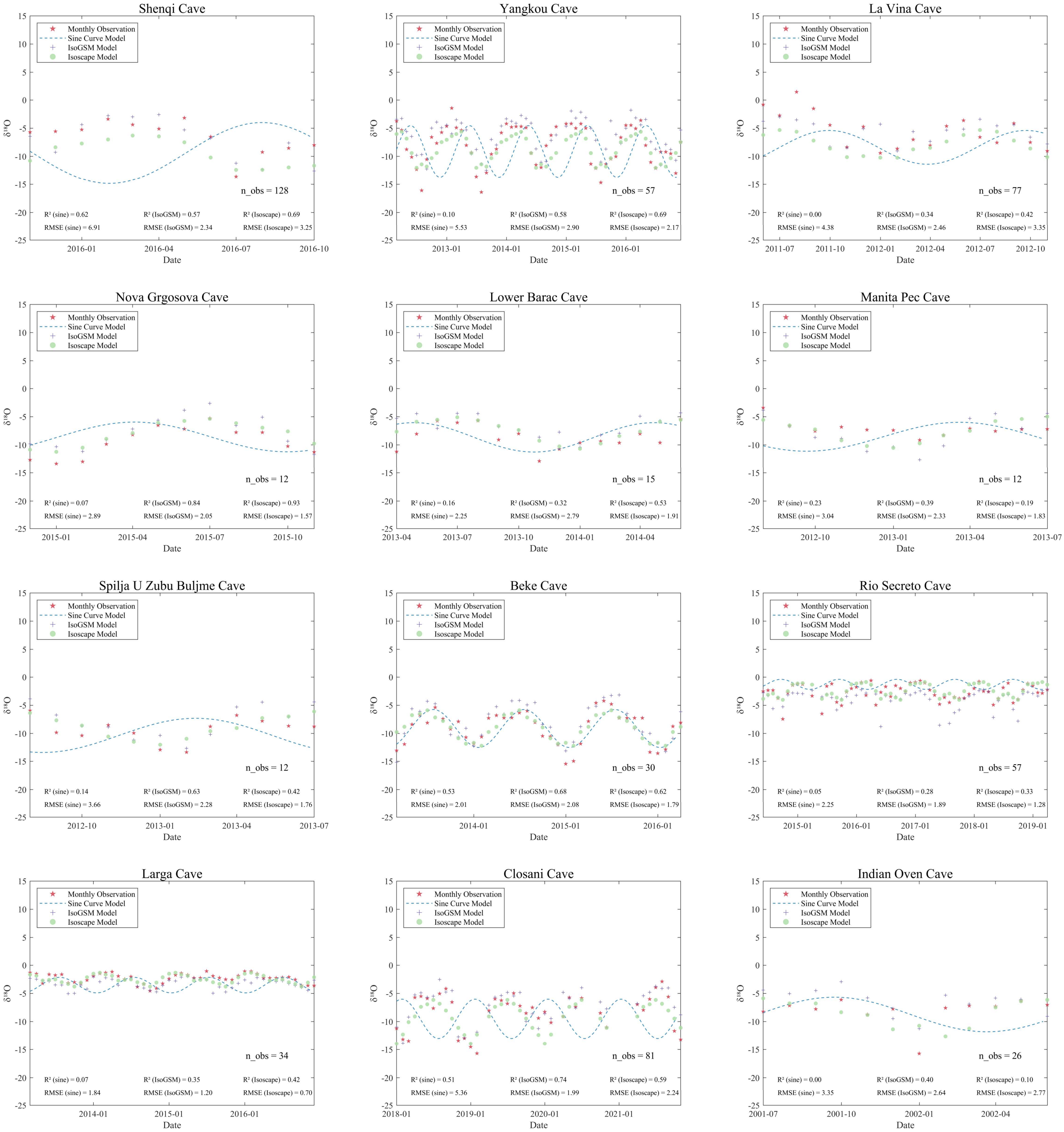
Shenqi Cave
n_obs = 128
R² (sine) = 0.62
RMSE (sine) = 6.91
R² (IsoGSM) = 0.57
RMSE (IsoGSM) = 2.34
R² (Isoscape) = 0.69
RMSE (Isoscape) = 3.25
Yangkou Cave
n_obs = 57
R² (sine) = 0.10
RMSE (sine) = 5.53
R² (IsoGSM) = 0.58
RMSE (IsoGSM) = 2.90
R² (Isoscape) = 0.69
RMSE (Isoscape) = 2.17
La Vina Cave
n_obs = 77
R² (sine) = 0.00
RMSE (sine) = 4.38
R² (IsoGSM) = 0.34
RMSE (IsoGSM) = 2.46
R² (Isoscape) = 0.42
RMSE (Isoscape) = 3.35
Nova Grgosova Cave
n_obs = 12
R² (sine) = 0.07
RMSE (sine) = 2.89
R² (IsoGSM) = 0.84
RMSE (IsoGSM) = 2.05
R² (Isoscape) = 0.93
RMSE (Isoscape) = 1.57
Lower Barac Cave
n_obs = 15
R² (sine) = 0.16
RMSE (sine) = 2.25
R² (IsoGSM) = 0.32
RMSE (IsoGSM) = 2.79
R² (Isoscape) = 0.53
RMSE (Isoscape) = 1.91
Manita Pec Cave
n_obs = 12
R² (sine) = 0.23
RMSE (sine) = 3.04
R² (IsoGSM) = 0.39
RMSE (IsoGSM) = 2.33
R² (Isoscape) = 0.19
RMSE (Isoscape) = 1.83
Spilja U Zubu Buljme Cave
n_obs = 12
R² (sine) = 0.14
RMSE (sine) = 3.66
R² (IsoGSM) = 0.63
RMSE (IsoGSM) = 2.28
R² (Isoscape) = 0.42
RMSE (Isoscape) = 1.76
Beke Cave
n_obs = 30
R² (sine) = 0.53
RMSE (sine) = 2.01
R² (IsoGSM) = 0.68
RMSE (IsoGSM) = 2.08
R² (Isoscape) = 0.62
RMSE (Isoscape) = 1.79
Rio Secreto Cave
n_obs = 57
R² (sine) = 0.05
RMSE (sine) = 2.25
R² (IsoGSM) = 0.28
RMSE (IsoGSM) = 1.89
R² (Isoscape) = 0.33
RMSE (Isoscape) = 1.28
Larga Cave
n_obs = 34
R² (sine) = 0.07
RMSE (sine) = 1.84
R² (IsoGSM) = 0.35
RMSE (IsoGSM) = 1.20
R² (Isoscape) = 0.42
RMSE (Isoscape) = 0.70
Closani Cave
n_obs = 81
R² (sine) = 0.51
RMSE (sine) = 5.36
R² (IsoGSM) = 0.74
RMSE (IsoGSM) = 1.99
R² (Isoscape) = 0.59
RMSE (Isoscape) = 2.24
Indian Oven Cave
n_obs = 26
R² (sine) = 0.00
RMSE (sine) = 3.35
R² (IsoGSM) = 0.40
RMSE (IsoGSM) = 2.64
R² (Isoscape) = 0.10
RMSE (Isoscape) = 2.77
Monthly Observation
Sine Curve Model
IsoGSM Model
Isoscape Model
δ¹⁸O
Date

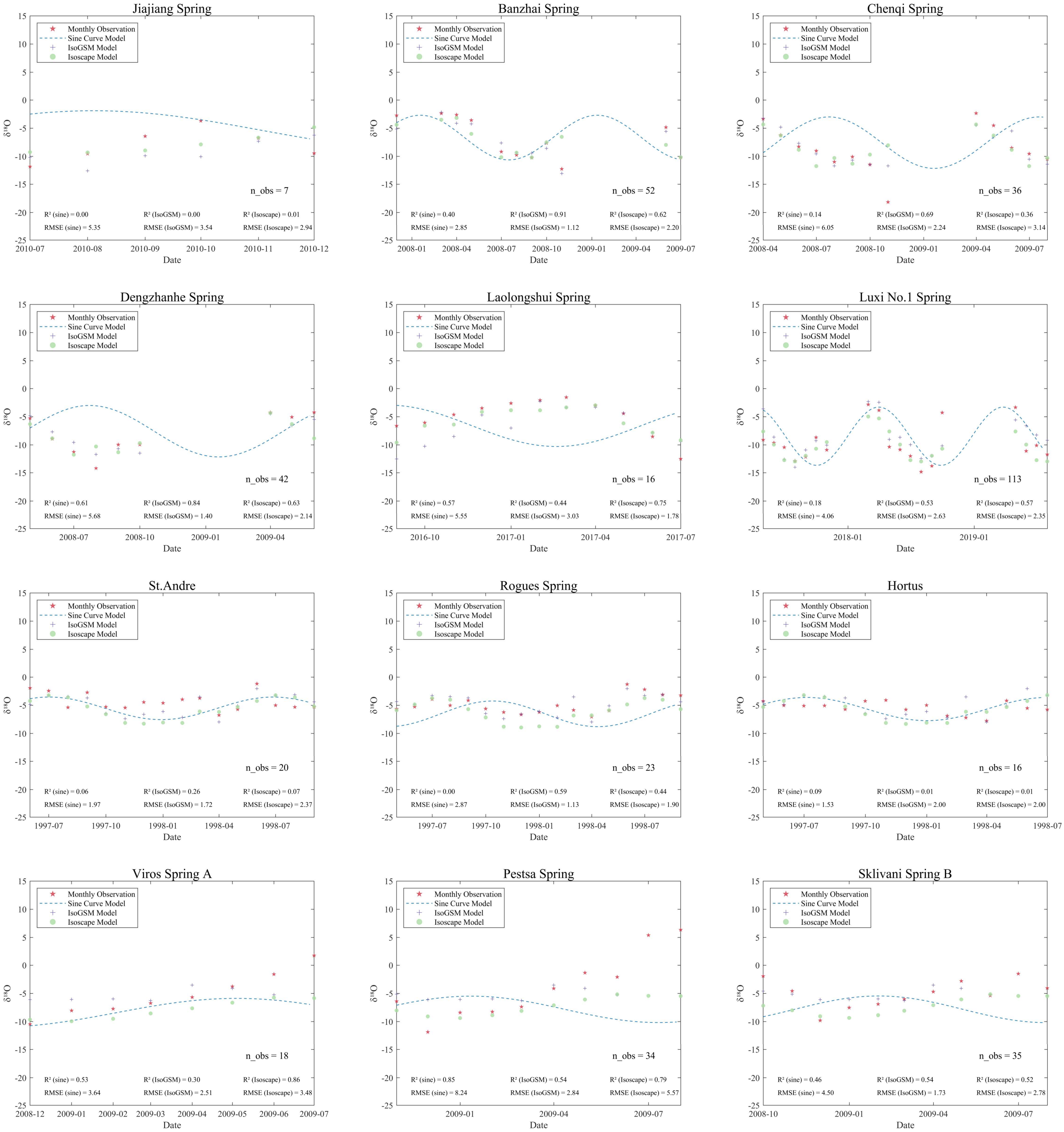
Jiajiang Spring
n_obs = 7
R² (sine) = 0.00 R² (IsoGSM) = 0.00 R² (Isoscape) = 0.01
RMSE (sine) = 5.35 RMSE (IsoGSM) = 3.54 RMSE (Isoscape) = 2.94
Banzhai Spring
n_obs = 52
R² (sine) = 0.40 R² (IsoGSM) = 0.91 R² (Isoscape) = 0.62
RMSE (sine) = 2.85 RMSE (IsoGSM) = 1.12 RMSE (Isoscape) = 2.20
Chenqi Spring
n_obs = 36
R² (sine) = 0.14 R² (IsoGSM) = 0.69 R² (Isoscape) = 0.36
RMSE (sine) = 6.05 RMSE (IsoGSM) = 2.24 RMSE (Isoscape) = 3.14
Dengzhanhe Spring
n_obs = 42
R² (sine) = 0.61 R² (IsoGSM) = 0.84 R² (Isoscape) = 0.63
RMSE (sine) = 5.68 RMSE (IsoGSM) = 1.40 RMSE (Isoscape) = 2.14
Laolongshui Spring
n_obs = 16
R² (sine) = 0.57 R² (IsoGSM) = 0.44 R² (Isoscape) = 0.75
RMSE (sine) = 5.55 RMSE (IsoGSM) = 3.03 RMSE (Isoscape) = 1.78
Luxi No.1 Spring
n_obs = 113
R² (sine) = 0.18 R² (IsoGSM) = 0.53 R² (Isoscape) = 0.57
RMSE (sine) = 4.06 RMSE (IsoGSM) = 2.63 RMSE (Isoscape) = 2.35
St.Andre
n_obs = 20
R² (sine) = 0.06 R² (IsoGSM) = 0.26 R² (Isoscape) = 0.07
RMSE (sine) = 1.97 RMSE (IsoGSM) = 1.72 RMSE (Isoscape) = 2.37
Rogues Spring
n_obs = 23
R² (sine) = 0.00 R² (IsoGSM) = 0.59 R² (Isoscape) = 0.44
RMSE (sine) = 2.87 RMSE (IsoGSM) = 1.13 RMSE (Isoscape) = 1.90
Hortus
n_obs = 16
R² (sine) = 0.09 R² (IsoGSM) = 0.01 R² (Isoscape) = 0.01
RMSE (sine) = 1.53 RMSE (IsoGSM) = 2.00 RMSE (Isoscape) = 2.00
Viros Spring A
n_obs = 18
R² (sine) = 0.53 R² (IsoGSM) = 0.30 R² (Isoscape) = 0.86
RMSE (sine) = 3.64 RMSE (IsoGSM) = 2.51 RMSE (Isoscape) = 3.48
Pestsa Spring
n_obs = 34
R² (sine) = 0.85 R² (IsoGSM) = 0.54 R² (Isoscape) = 0.79
RMSE (sine) = 8.24 RMSE (IsoGSM) = 2.84 RMSE (Isoscape) = 5.57
Sklivani Spring B
n_obs = 35
R² (sine) = 0.46 R² (IsoGSM) = 0.54 R² (Isoscape) = 0.52
RMSE (sine) = 4.50 RMSE (IsoGSM) = 1.73 RMSE (Isoscape) = 2.78
Monthly Observation
Sine Curve Model
IsoGSM Model
Isoscape Model
δ¹⁸O
Date

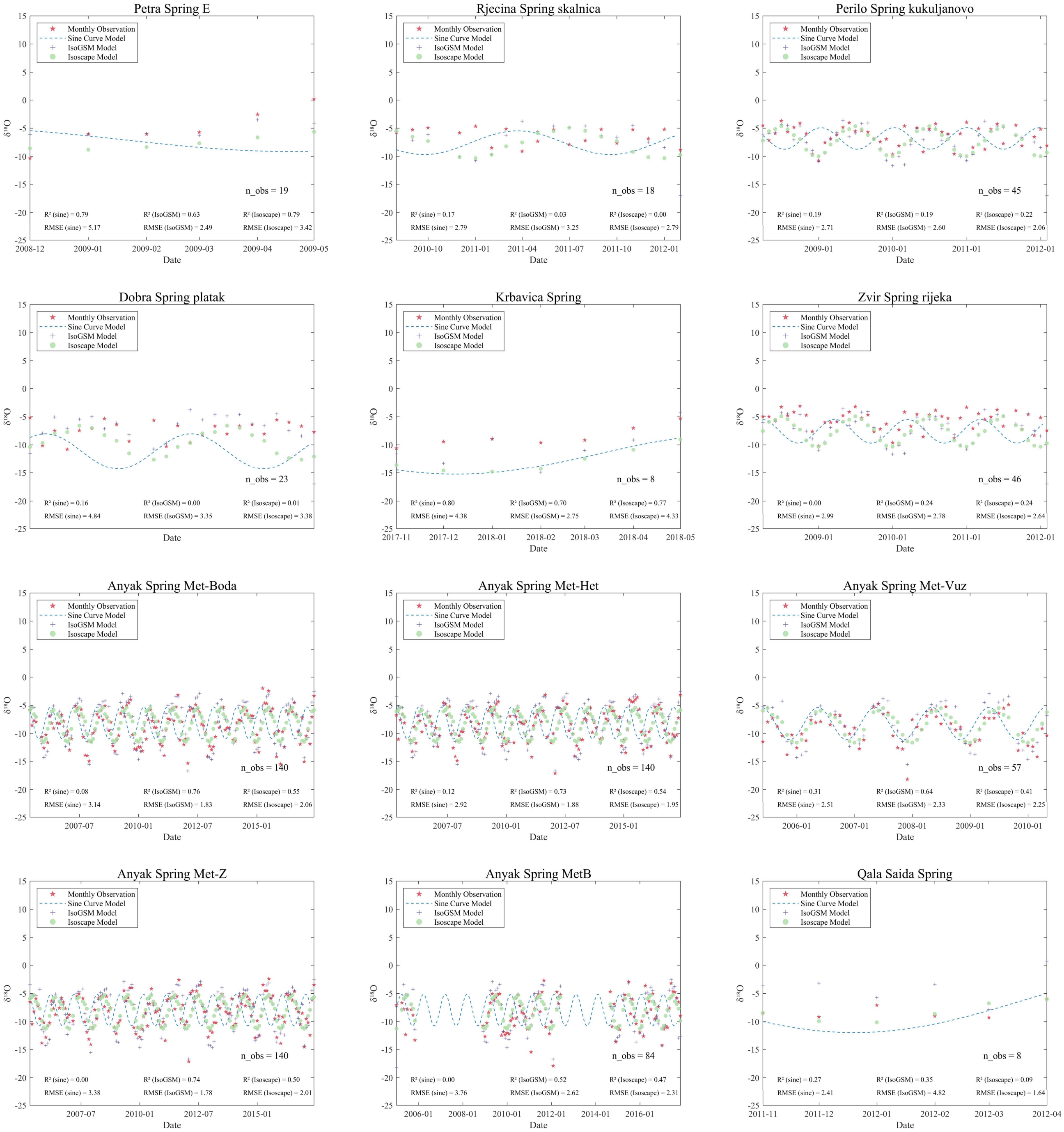

Petra Spring E
Monthly Observation
Sine Curve Model
IsoGSM Model
Isoscape Model
n_obs = 19
R² (sine) = 0.79
R² (IsoGSM) = 0.63
R² (Isoscape) = 0.79
RMSE (sine) = 5.17
RMSE (IsoGSM) = 2.49
RMSE (Isoscape) = 3.42
Rjecina Spring skalnica
n_obs = 18
R² (sine) = 0.17
R² (IsoGSM) = 0.03
R² (Isoscape) = 0.00
RMSE (sine) = 2.79
RMSE (IsoGSM) = 3.25
RMSE (Isoscape) = 2.79
Perilo Spring kukuljanovo
n_obs = 45
R² (sine) = 0.19
R² (IsoGSM) = 0.19
R² (Isoscape) = 0.22
RMSE (sine) = 2.71
RMSE (IsoGSM) = 2.60
RMSE (Isoscape) = 2.06
Dobra Spring platak
n_obs = 23
R² (sine) = 0.16
R² (IsoGSM) = 0.00
R² (Isoscape) = 0.01
RMSE (sine) = 4.84
RMSE (IsoGSM) = 3.35
RMSE (Isoscape) = 3.38
Krbavica Spring
n_obs = 8
R² (sine) = 0.80
R² (IsoGSM) = 0.70
R² (Isoscape) = 0.77
RMSE (sine) = 4.38
RMSE (IsoGSM) = 2.75
RMSE (Isoscape) = 4.33
Zvir Spring rijeka
n_obs = 46
R² (sine) = 0.00
R² (IsoGSM) = 0.24
R² (Isoscape) = 0.24
RMSE (sine) = 2.99
RMSE (IsoGSM) = 2.78
RMSE (Isoscape) = 2.64
Anyak Spring Met-Boda
n_obs = 140
R² (sine) = 0.08
R² (IsoGSM) = 0.76
R² (Isoscape) = 0.55
RMSE (sine) = 3.14
RMSE (IsoGSM) = 1.83
RMSE (Isoscape) = 2.06
Anyak Spring Met-Het
n_obs = 140
R² (sine) = 0.12
R² (IsoGSM) = 0.73
R² (Isoscape) = 0.54
RMSE (sine) = 2.92
RMSE (IsoGSM) = 1.88
RMSE (Isoscape) = 1.95
Anyak Spring Met-Vuz
n_obs = 57
R² (sine) = 0.31
R² (IsoGSM) = 0.64
R² (Isoscape) = 0.41
RMSE (sine) = 2.51
RMSE (IsoGSM) = 2.33
RMSE (Isoscape) = 2.25
Anyak Spring Met-Z
n_obs = 140
R² (sine) = 0.00
R² (IsoGSM) = 0.74
R² (Isoscape) = 0.50
RMSE (sine) = 3.38
RMSE (IsoGSM) = 1.78
RMSE (Isoscape) = 2.01
Anyak Spring MetB
n_obs = 84
R² (sine) = 0.00
R² (IsoGSM) = 0.52
R² (Isoscape) = 0.47
RMSE (sine) = 3.76
RMSE (IsoGSM) = 2.62
RMSE (Isoscape) = 2.31
Qala Saida Spring
n_obs = 8
R² (sine) = 0.27
R² (IsoGSM) = 0.35
R² (Isoscape) = 0.09
RMSE (sine) = 2.41
RMSE (IsoGSM) = 4.82
RMSE (Isoscape) = 1.64
Date
δ¹⁸O

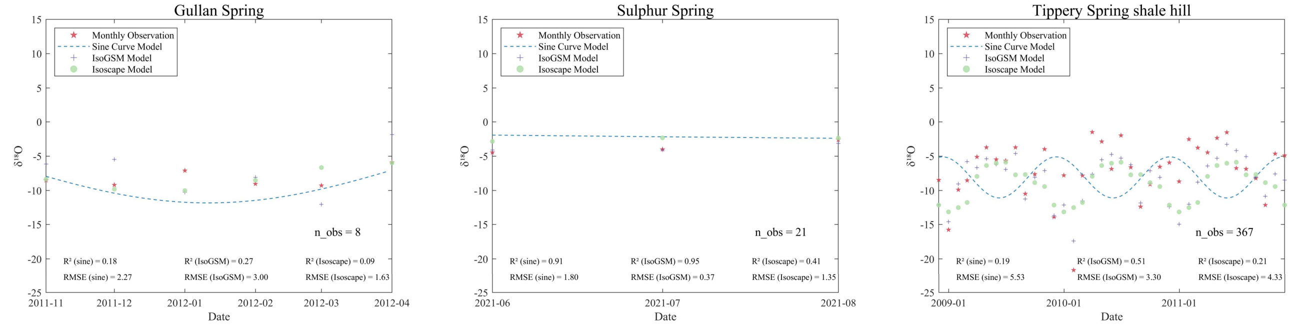

Figure S1: Time series comparison of modelled and observed monthly $\delta^{18}O$ in precipitation at 51 sites. Observations (red stars) are compared with estimates from the Sine Curve model (dashed blue line), IsoGSM (purple crosses), and the Isoscape model (green circles). Each panel shows the number of monthly observations (n.obs) and model performance statistics (R^2 and RMSE).

S2 Evaluation of different precipitation δ^2H data

Fig.S2 presents the similar performance trends for δ^2H predictions. The IsoGSM achieves the lowest RMSE median (~17 ‰) with a relatively narrow spread, reflecting the most accurate and consistent predictions. The Isoscape model follows closely with a slightly higher RMSE (~19 ‰) and a greater variability. The Sine Curve model shows the highest RMSE median value (~29 ‰) and the broadest RMSE distribution. For R^2, there is a slight shift in performance ranking compared to $\delta^{18}O$. The Isoscape model has the highest R^2 value (~0.5). The IsoGSM model has a lower R^2 (~0.4) with a more balanced distribution. The Sine Curve model exhibits the poorest fit with a median R^2 below 0.2.

Fig.S3 presents δ^2H time series comparisons between observations and simulations from three models at four sites: Heshang Cave, Yongxing Cave, Krbavica Spring and Laolongshui Spring(comparion for other sites shown in Figure S4). Similarly, the Sine Curve model shows the poorest agreement with observations at Heshang Cave, Yongxing Cave and Krbavica Spring as reflected by low R^2 values of 0.37, 0.57 and 0.1 respectively and high RMSEs (up to 50.11 ‰). Although it shows relativley higher R^2 values of 0.85 at Laolongshui Spring, its corresponding large RMSE value of 46.55 reveals substantial absolute predictive errors.

The IsoGSM model shows the best performance at Heshang Cave and Yongxing Cave, with the highest R2 (0.8 and 0.82) and lowest RMSE (15.53 ‰ and 10.56 ‰). These highlight IsoGSM model's strong predictive accuracy in tracking δ^2H variability at both sites.

At Krbavica Spring, the IsoGSM and Isoscape exhibit comparable performance in terms of correlation with R2 values of 0.71 and 0.7. However, IsoGSM shows a lower RMSE (21.3 ‰) compared to Isoscape (35.21 ‰), indicating that although both models reproduce the temporal variation similarly, IsoGSM offers more precise estimates of δ^2H magnitudes.

At Laolongshui Spring (Fig.S3(d)), the Isoscape model outperforms the IsoGSM model and Sine Curve model with the highest R^2 and lowest RMSE values.

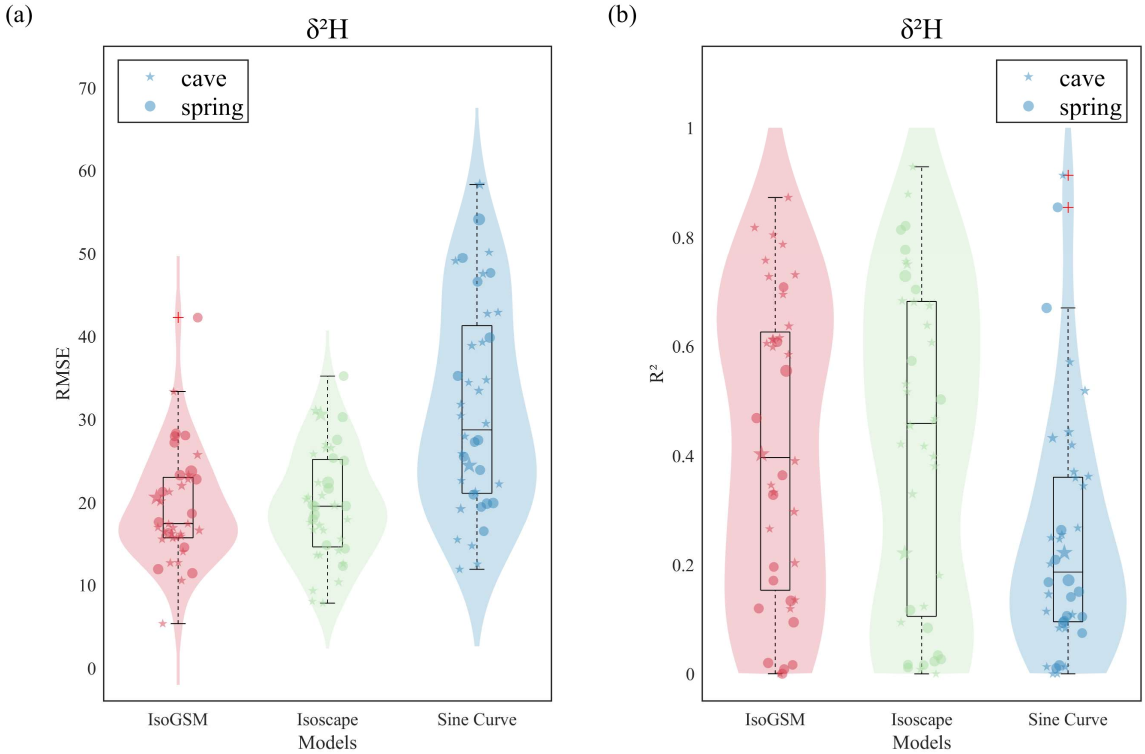

Figure S2: Statistical comparison of three model performance for δ2H in precipitation at cave (stars) and springs sites (circles). (a)Root Mean Square Error (RMSE); (b) Coefficient of determination (R^2). Violin plots show the distribution of performance metrics for each model: IsoGSM (red), Isoscape (green), and Sine Curve (blue). Boxplots within violin indicate the median, interquartile range and outliers. Lower RMSE and higher R2 indicate better model performance.

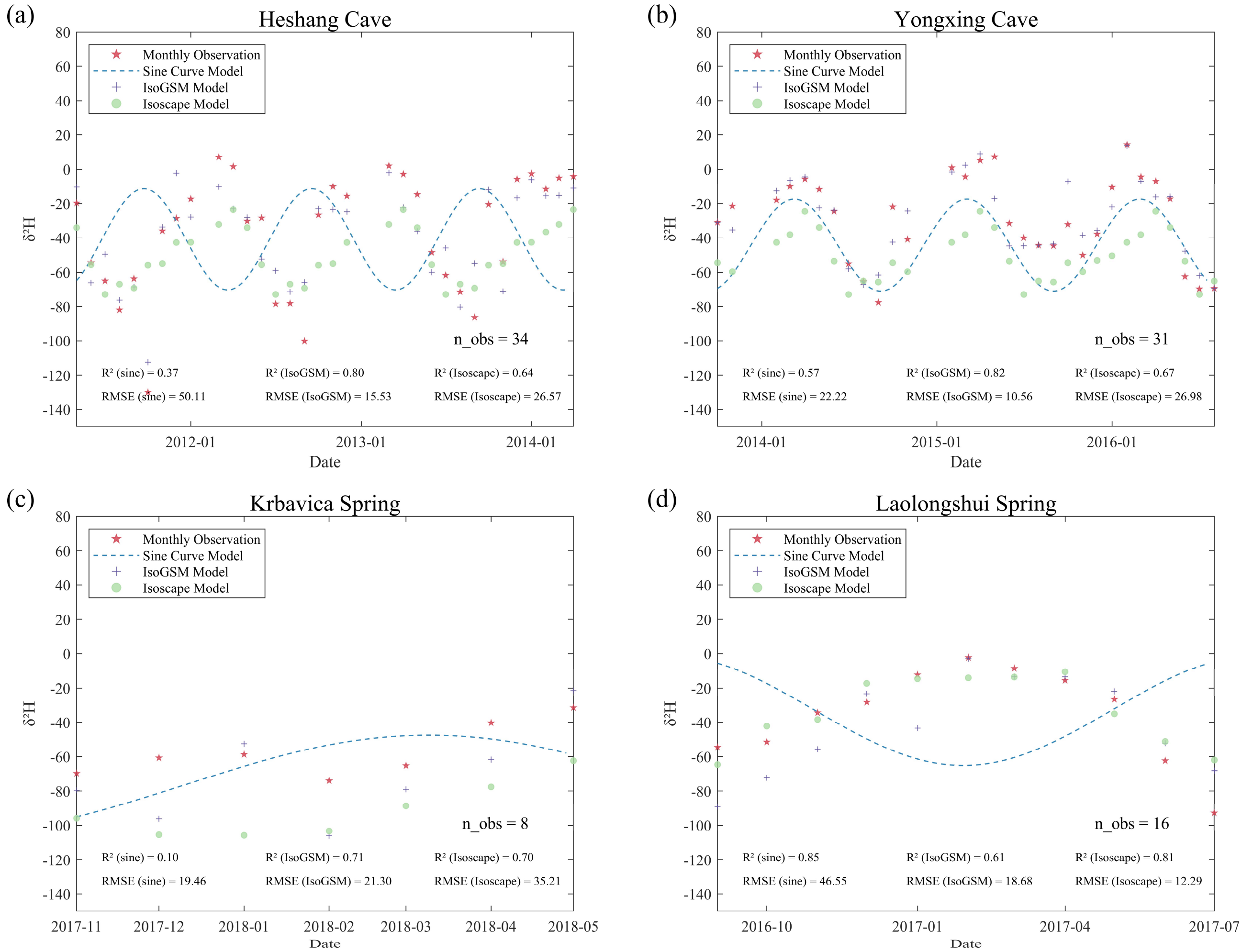

130 Figure S3: Time series comparison of modelled and observed monthly δ^2H in precipitation at two cave sites (a–b) and two spring sites (c–d). Observations (red stars) are compared with estimates from the Sine Curve model (dashed blue line), IsoGSM (purple crosses), and the Isoscape model (green circles). Each panel shows the number of monthly observations (n.obs) and model performance statistics (R^2 and RMSE).

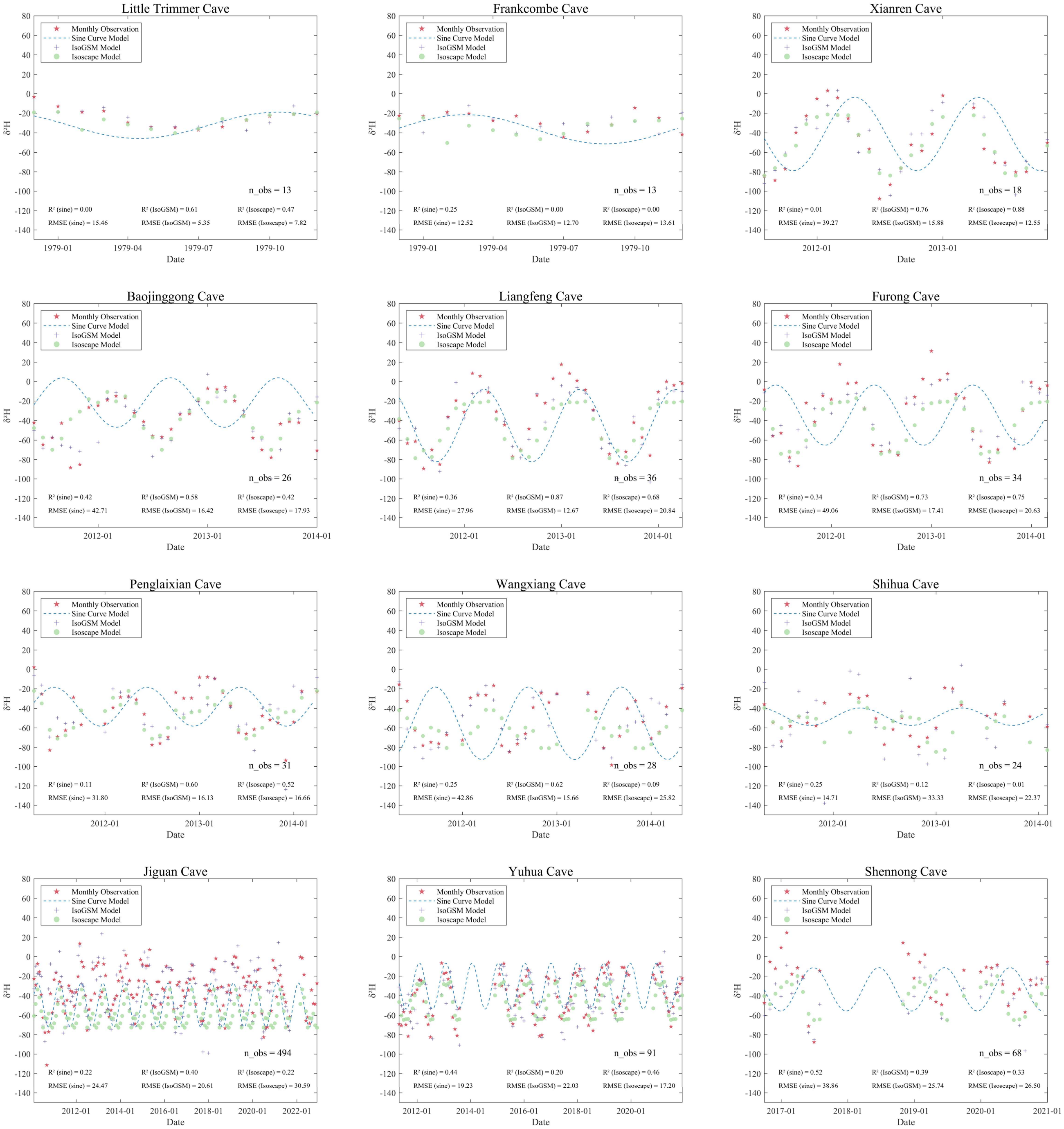
Little Trimmer Cave
n_obs = 13
R² (sine) = 0.00 R² (IsoGSM) = 0.61 R² (Isoscape) = 0.47
RMSE (sine) = 15.46 RMSE (IsoGSM) = 5.35 RMSE (Isoscape) = 7.82
Frankcombe Cave
n_obs = 13
R² (sine) = 0.25 R² (IsoGSM) = 0.00 R² (Isoscape) = 0.00
RMSE (sine) = 12.52 RMSE (IsoGSM) = 12.70 RMSE (Isoscape) = 13.61
Xianren Cave
n_obs = 18
R² (sine) = 0.01 R² (IsoGSM) = 0.76 R² (Isoscape) = 0.88
RMSE (sine) = 39.27 RMSE (IsoGSM) = 15.88 RMSE (Isoscape) = 12.55
Baojinggong Cave
n_obs = 26
R² (sine) = 0.42 R² (IsoGSM) = 0.58 R² (Isoscape) = 0.42
RMSE (sine) = 42.71 RMSE (IsoGSM) = 16.42 RMSE (Isoscape) = 17.93
Liangfeng Cave
n_obs = 36
R² (sine) = 0.36 R² (IsoGSM) = 0.87 R² (Isoscape) = 0.68
RMSE (sine) = 27.96 RMSE (IsoGSM) = 12.67 RMSE (Isoscape) = 20.84
Furong Cave
n_obs = 34
R² (sine) = 0.34 R² (IsoGSM) = 0.73 R² (Isoscape) = 0.75
RMSE (sine) = 49.06 RMSE (IsoGSM) = 17.41 RMSE (Isoscape) = 20.63
Penglaixian Cave
n_obs = 31
R² (sine) = 0.11 R² (IsoGSM) = 0.60 R² (Isoscape) = 0.52
RMSE (sine) = 31.80 RMSE (IsoGSM) = 16.13 RMSE (Isoscape) = 16.66
Wangxiang Cave
n_obs = 28
R² (sine) = 0.25 R² (IsoGSM) = 0.62 R² (Isoscape) = 0.09
RMSE (sine) = 42.86 RMSE (IsoGSM) = 15.66 RMSE (Isoscape) = 25.82
Shihua Cave
n_obs = 24
R² (sine) = 0.25 R² (IsoGSM) = 0.12 R² (Isoscape) = 0.01
RMSE (sine) = 14.71 RMSE (IsoGSM) = 33.33 RMSE (Isoscape) = 22.37
Jiguan Cave
n_obs = 494
R² (sine) = 0.22 R² (IsoGSM) = 0.40 R² (Isoscape) = 0.22
RMSE (sine) = 24.47 RMSE (IsoGSM) = 20.61 RMSE (Isoscape) = 30.59
Yuhua Cave
n_obs = 91
R² (sine) = 0.44 R² (IsoGSM) = 0.20 R² (Isoscape) = 0.46
RMSE (sine) = 19.23 RMSE (IsoGSM) = 22.03 RMSE (Isoscape) = 17.20
Shennong Cave
n_obs = 68
R² (sine) = 0.52 R² (IsoGSM) = 0.39 R² (Isoscape) = 0.33
RMSE (sine) = 38.86 RMSE (IsoGSM) = 25.74 RMSE (Isoscape) = 26.50
Monthly Observation
Sine Curve Model
IsoGSM Model
Isoscape Model
δ²H
Date


Shenqi Cave
Monthly Observation
Sine Curve Model
IsoGSM Model
Isoscape Model
n_obs = 128
R² (sine) = 0.43
R² (IsoGSM) = 0.61
R² (Isoscape) = 0.75
RMSE (sine) = 58.29
RMSE (IsoGSM) = 20.14
RMSE (Isoscape) = 31.05
Yangkou Cave
n_obs = 57
R² (sine) = 0.08
R² (IsoGSM) = 0.64
R² (Isoscape) = 0.68
RMSE (sine) = 47.50
RMSE (IsoGSM) = 23.28
RMSE (Isoscape) = 20.38
La Vina Cave
n_obs = 77
R² (sine) = 0.15
R² (IsoGSM) = 0.30
R² (Isoscape) = 0.38
RMSE (sine) = 33.45
RMSE (IsoGSM) = 16.59
RMSE (Isoscape) = 19.67
Nova Grgosova Cave
n_obs = 12
R² (sine) = 0.91
R² (IsoGSM) = 0.79
R² (Isoscape) = 0.93
RMSE (sine) = 34.43
RMSE (IsoGSM) = 14.01
RMSE (Isoscape) = 8.03
Lower Barac Cave
n_obs = 15
R² (sine) = 0.27
R² (IsoGSM) = 0.27
R² (Isoscape) = 0.46
RMSE (sine) = 25.87
RMSE (IsoGSM) = 22.79
RMSE (Isoscape) = 15.53
Manita Pec Cave
n_obs = 12
R² (sine) = 0.20
R² (IsoGSM) = 0.35
R² (Isoscape) = 0.12
RMSE (sine) = 22.64
RMSE (IsoGSM) = 21.27
RMSE (Isoscape) = 16.59
Spilja U Zubu Buljme Cave
n_obs = 12
R² (sine) = 0.36
R² (IsoGSM) = 0.61
R² (Isoscape) = 0.42
RMSE (sine) = 30.42
RMSE (IsoGSM) = 15.72
RMSE (Isoscape) = 13.57
Beke Cave
n_obs = 30
R² (sine) = 0.08
R² (IsoGSM) = 0.69
R² (Isoscape) = 0.61
RMSE (sine) = 34.73
RMSE (IsoGSM) = 16.96
RMSE (Isoscape) = 14.14
Larga Cave
n_obs = 24
R² (sine) = 0.00
R² (IsoGSM) = 0.14
R² (Isoscape) = 0.18
RMSE (sine) = 11.90
RMSE (IsoGSM) = 16.21
RMSE (Isoscape) = 9.32
Closani Cave
n_obs = 39
R² (sine) = 0.01
R² (IsoGSM) = 0.73
R² (Isoscape) = 0.53
RMSE (sine) = 29.50
RMSE (IsoGSM) = 17.39
RMSE (Isoscape) = 17.58
Wasseralmquelle(B)
n_obs = 34
R² (sine) = 0.67
R² (IsoGSM) = 0.02
R² (Isoscape) = 0.02
RMSE (sine) = 49.44
RMSE (IsoGSM) = 11.43
RMSE (Isoscape) = 17.96
Jiajiang Spring
n_obs = 7
R² (sine) = 0.01
R² (IsoGSM) = 0.02
R² (Isoscape) = 0.01
RMSE (sine) = 47.61
RMSE (IsoGSM) = 28.32
RMSE (Isoscape) = 25.34
δ²H
Date

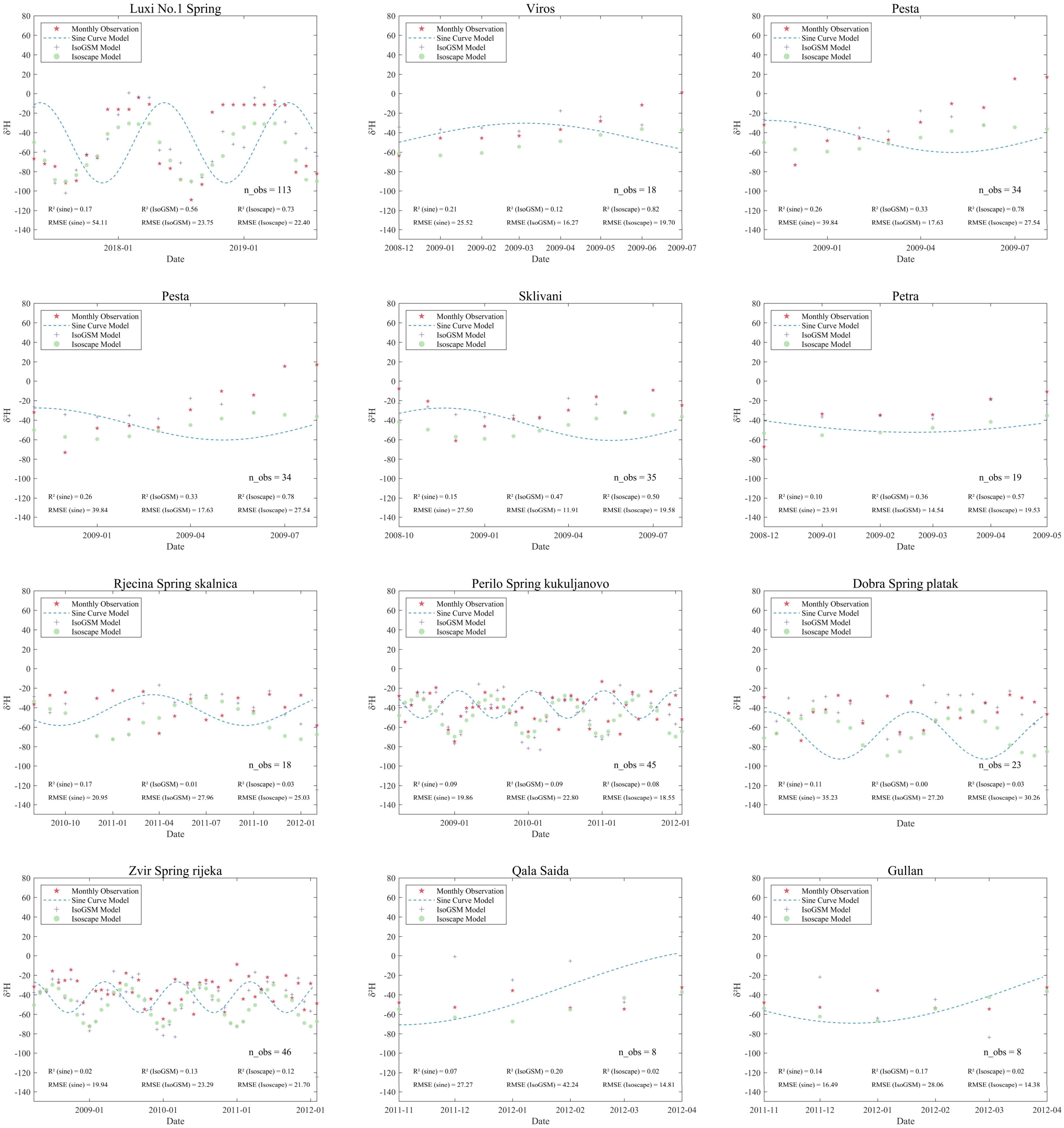

Figure S4: Time series comparison of modelled and observed monthly δ^2H in precipitation at 36 sites are compared with estimates from the Sine Curve model (dashed blue line), IsoGSM (purple crosses), and the Isoscape model (green circles). Each panel shows the number of monthly observations (n.obs) and model performance statistics (R^2 and RMSE).

S3 Complete list of sites included in the WoKaS-Iso database

Table S1: Karst springs included in the WoKaS-Iso database

ID	Country	Name	Latitude	Longitude	References
AT-S-0001	Austria	LTER-Zoebelboden	47.8381	14.4411	Martin Kralic (Olarinoye et al., 2020)
AT-S-0002	Austria	Wasseralmquelle(A)	47.7329	15.6456	(eHYD, 2025) (Maloszewski et al., 2002)
AT-S-0003	Austria	Siebenquellen	47.6837	15.5658	(eHYD, 2025) (Maloszewski et al., 2002)
AT-S-0004	Austria	Lappenbachquelle	46.7245	13.0409	(eHYD, 2025) Probost et al., 1998)
AT-S-0005	Austria	Hammerbachquelle	47.2100	15.3500	(eHYD, 2025)
AT-S-0006	Austria	Schreiende_Brunnen	47.4300	12.5800	(eHYD, 2025) (Papesch and Rank, 1998; Humer et al., 2015)
AT-S-0007	Austria	Gerstenboedenquelle	47.2600	9.7700	(eHYD, 2025) (Kralik, 2015)
AT-S-0008	Austria	Wasseralmquelle(B)	47.7351	15.6486	(Olarinoye et al., 2020) (eHYD, 2025) (Wieselthaler, 2006)
AT-S-0009	Austria	Baumbachquelle(Gosau)	47.5444	13.5093	Martin Kralik
AT-S-0010	Austria	BrunnenbachQ (Gosau)	47.5453	13.5074	Martin Kralik
AT-S-0011	Austria	Jägerwaldquelle(Gosau)	47.5863	13.5732	Martin Kralik
AT-S-0012	Austria	Brunnbach Nebenquelle (Gosau)	47.5500	13.5201	Martin Kralik
AT-S-0013	Austria	Gosauseequelle (Gosau)	47.5228	13.5167	Martin Kralik
AT-S-0014	Austria	Brielbachquelle(Gosau)	47.5686	13.5509	Martin Kralik
AT-S-0015	Austria	Waldbachursprung (Hallstatt)	47.5430	13.6074	Martin Kralik (eHYD, 2025)
AT-S-0016	Austria	Hirschbrunn (Hallstatt)	47.5467	13.6584	Martin Kralik (eHYD, 2025)
AT-S-0017	Austria	Bühlerbachursprung (Obertraun)	47.5564	13.7265	Martin Kralik

ID	Country	Name	Latitude	Longitude	References
AT-S-0018	Austria	Ödensee - Kaltwassertrichter (Pichl-Kainisch)	47.5636	13.8257	Martin Kralik (eHYD, 2025)
AT-S-0019	Austria	Meeräuglquelle (Bögreinalm) (Sankt Andrä im Lungau)	47.4696	13.5297	Martin Kralik
AT-S-0020	Austria	Koppenbrüllerquellen(Obertraun)	47.5568	13.7257	Martin Kralik
AT-S-0021	Austria	Groedig	47.7400	12.9900	(Reischer et al., 2015)
AT-S-0022	Austria	Fuerstenbrunner_Quellhoehe	47.7383	12.9947	(Reischer et al., 2015)
AT-S-0023	Austria	Veitlbruchquelle	47.7330	12.9730	(Reischer et al., 2015)
AT-S-0024	Austria	Halmquelle	47.7339	13.0359	(Reischer et al., 2015)
AT-S-0025	Austria	Glanegg-1-Quelle	47.7444	13.0081	(Reischer et al., 2015)
AT-S-0026	Austria	Hofingerquelle	47.5927	12.2310	(Joanneum Research, 2008)
AT-S-0027	Austria	Fieberbrunn	47.4300	12.5800	(Papesch and Rank, 1998; Humer et al., 2015)
CH-S-0001	Switzerland	Rappenfluh	47.4868	7.6664	Andreas Hartmann (Olarinoye et al., 2020)
CN-S-0001	China	Jiajiang Spring	29.6766	106.3014	Xiao Qiong
CN-S-0002	China	Bei Wenquan Hot Spring	29.8491	106.4186	Xiao Qiong
CN-S-0003	China	Qiaocun Spring	25.056	107.5451	Xiao Qiong
CN-S-0004	China	Gantianba Spring	25.0874	107.6539	Xiao Qiong
CN-S-0005	China	Xiaolongdong Spring	25.1789	107.7198	Xiao Qiong
CN-S-0006	China	Banzhai Spring	25.2188	108.0078	(Zhao et al., 2018)
CN-S-0007	China	Chenqi Spring	26.2638	105.7682	(Zhao et al., 2018)
CN-S-0008	China	Dengzhanhe Spring	26.2506	105.7682	(Zhao et al., 2018)
CN-S-0009	China	Qingshuitan Spring	25.1407	102.7462	(Huang et al., 2015)
CN-S-0010	China	Hunshuitan Spring	25.1411	102.7463	(Huang et al., 2015)
CN-S-0011	China	Xiaoshuitan Spring	26.8908	100.2323	(Huang et al., 2015)
CN-S-0012	China	Baotu Spring	36.6612	117.0159	(Guo et al., 2019)
CN-S-0013	China	Heihu Spring	36.6626	117.0332	(Guo et al., 2019)
CN-S-0014	China	Jinlongdong Spring	25.7161	101.3281	(Lyu et al., 2023)
CN-S-0015	China	Chaoshuidong spring	30.7354	111.0869	(Guo et al., 2022)
CN-S-0016	China	Wulongdong Spring	31.2508	110.8921	(Luo et al., 2018) (Olarinoye et al., 2020)

ID	Country	Name	Latitude	Longitude	References
CN-S-0017	China	Shuimoxi Spring	31.3262	110.7978	(Luo et al., 2016)
CN-S-0018	China	Xiangshuidong Spring	31.3400	110.7970	(Luo et al., 2016)
CN-S-0019	China	Bailongquan Spring	31.2394	110.8635	(Luo et al., 2018)
CN-S-0020	China	Heilongquan Spring	31.2402	110.8681	(Luo et al., 2018)
CN-S-0021	China	Yunlongdong Spring	31.2517	110.8970	(Luo et al., 2018)
CN-S-0022	China	Qinglongkou Spring	31.4256	111.0116	(Luo et al., 2018)
CN-S-0023	China	Miaopingquan Spring	30.7798	110.8990	(Wang et al., 2022)
CN-S-0024	China	Yuquandong Spring	30.7380	110.9183	(Wang et al., 2022)
CN-S-0025	China	Migongquan Spring	30.7206	110.9132	(Wang et al., 2022)
CN-S-0026	China	Changliushui C1 Spring	25.0281	110.3711	Wang Zhijun
CN-S-0027	China	Beidiping Spring	25.1824	110.5607	Huang Fen
CN-S-0028	China	Laolongshui Spring	25.1737	110.5560	Huang Fen
CN-S-0029	China	Yaji S31 Spring	25.2458	110.3779	Yu Shi
CN-S-0030	China	Luxi No.1 Spring	24.4678	103.8444	Pu Junbing
CN-S-0031	China	Luxi No.2 Spring	24.4678	103.8444	Pu Junbing
CN-S-0032	China	Luxi No.3 Spring	24.4678	103.8444	Pu Junbing
CN-S-0033	China	Nandong underground river	23.6500	103.2900	Pu Junbing (Olarinoye et al., 2020)
CN-S-0034	China	Guancun underground river	24.8694	109.3353	Pu Junbing (Olarinoye et al., 2020)
CN-S-0035	China	Babu Spring	26.8502	105.7774	(Ren et al., 2021, 2022)
CZ-S-0001	Czech Republic	Jedovnicky Potok	49.3083	16.6922	Pavel Pracný/Jiří Faimon/Marek Lang
DE-S-0001	Germany	Schwarbachloch	47.6392	12.8472	Garvelmann/Kunstmann
DE-S-0002	Germany	Gletscherquellen	47.6070	12.8808	Garvelmann/Kunstmann
DE-S-0003	Germany	Klauswandl	47.5693	12.8021	Garvelmann/Kunstmann
DE-S-0004	Germany	Obere Wimbachquellen	47.5955	12.9165	Garvelmann/Kunstmann
DE-S-0005	Germany	Schapbach	47.5832	12.9530	Garvelmann/Kunstmann
DE-S-0006	Germany	Schwarzbrunn	47.5859	12.8295	Garvelmann/Kunstmann
DE-S-0007	Germany	Staumauer_unten	47.5846	12.9066	Garvelmann/Kunstmann
DE-S-0008	Germany	Wasserversorgung_Bgd	47.5848	12.9064	Garvelmann/Kunstmann
DE-S-0009	Germany	Tunnel Spring	47.4442	11.0415	Goldscheider

ID	Country	Name	Latitude	Longitude	References
DE-S-0010	Germany	Gorge entrance Spring	47.4497	11.0477	Goldscheider
DE-S-0011	Germany	Rotgraben Spring	47.4510	11.0495	Goldscheider
DE-S-0012	Germany	Mariensprung	47.4393	11.0312	Goldscheider
DE-S-0013	Germany	Hammersbachquelle	47.4393	11.0312	Goldscheider
DE-S-0014	Germany	H3	47.4393	11.0312	Goldscheider
DE-S-0015	Germany	H4	47.4393	11.0312	Goldscheider
ES-S-0001	Spain	Benaojan (Spring S-2)	36.7151	-5.2452	Andreo/ Mudarra (Olarinoye et al., 2020)
ES-S-0002	Spain	Genal	36.6403	-5.1184	Andreo/ Mudarra (Olarinoye et al., 2020)
ES-S-0003	Spain	Canamero	36.8931	-4.9976	Andreo/ Mudarra (Olarinoye et al., 2020)
ES-S-0004	Spain	Canamero overflow	36.8738	-5.0105	Andreo/ Mudarra (Olarinoye et al., 2020)
ES-S-0005	Spain	Algarrobal	36.6713	-5.4459	(Marín et al., 2021; Antonio and Fornell, 2020)
ES-S-0006	Spain	Pileta	36.6646	-5.2805	Andreo/ Mudarra
ES-S-0007	Spain	Verde	36.6721	-5.0255	Andreo/ Mudarra
ES-S-0008	Spain	Grande	36.7217	-4.9378	Andreo/ Mudarra
ES-S-0009	Spain	Jorox	36.7323	-4.8906	Andreo/ Mudarra
ES-S-0010	Spain	9_Canos	36.6813	-5.4454	Andreo/ Mudarra
ES-S-0011	Spain	Arroyomolinos	36.8102	-5.3734	Andreo/ Mudarra
ES-S-0012	Spain	Benamahoma	36.7677	-5.4628	Andreo/ Mudarra
ES-S-0013	Spain	Bocaleones	36.7677	-5.4628	Andreo/ Mudarra
ES-S-0014	Spain	Villanueva del Rosario	36.9855	-4.3554	(Mudarra Martínez, 2012)
ES-S-0015	Spain	Canamero	36.8914	-4.9998	(Barberá-Fornell, 2014)
ES-S-0016	Spain	Carrizal	36.8712	-5.0444	(Barberá-Fornell, 2014)
ES-S-0017	Spain	El Burgo	36.7780	-5.9835	(Barberá-Fornell, 2014)
ES-S-0018	Spain	Hierbabuena	36.7742	-5.9948	(Barberá-Fornell, 2014)
FR-S-0001	France	Cents-Fonts	43.7598	3.6241	Ladouche (Olarinoye et al., 2020)
FR-S-0002	France	Cernon	43.9752	3.1456	(Plagnes, 1997)

ID	Country	Name	Latitude	Longitude	References
					(Olarinoye et al., 2020)
FR-S-0003	France	Durzon	43.9909	3.2617	(Plagnes, 1997)
					(Olarinoye et al., 2020)
FR-S-0004	France	Esperelle	44.1210	3.2085	(Plagnes, 1997)
					(Olarinoye et al., 2020)
FR-S-0005	France	Homede	44.0769	3.0605	(Plagnes, 1997)
					(Olarinoye et al., 2020)
FR-S-0006	France	Boundou	44.0667	3.0481	(Plagnes, 1997)
					(Olarinoye et al., 2020)
FR-S-0007	France	St. Andre	43.6930	3.6010	(Aquilina et al., 2006)
FR-S-0008	France	Rogues	43.8790	3.6000	(Aquilina et al., 2006)
FR-S-0009	France	Hortus	43.8290	3.7980	(Aquilina et al., 2006)
FR-S-0010	France	Fontanilles	43.7529	3.6233	Ladouche
					(Aquilina et al., 2006)
FR-S-0011	France	Bueges	43.8133	3.5910	Ladouche
					(Aquilina et al., 2006)
FR-S-0012	France	Lamalou	43.8230	3.8010	Ladouche
					(Aquilina et al., 2006)
FR-S-0013	France	Lavencou	44.0356	3.0422	(Plagnes, 1997)
FR-S-0014	France	Mouline	43.9921	3.0942	(Plagnes, 1997)
FR-S-0015	France	Verneau	46.9785	6.0057	(Charlier J.-B. et al, 2024)
FR-S-0016	France	Lison	46.9654	6.0113	(Charlier J.-B. et al, 2024)
FR-S-0017	France	Loue	47.0107	6.2998	(Charlier J.-B. et al, 2024)
FR-S-0018	France	Baume Archée	47.0295	6.2847	(Charlier J.-B. et al, 2024)
FR-S-0019	France	Ecoutot	47.0991	6.0388	(Charlier J.-B. et al, 2024)
FR-S-0020	France	Maine	47.0946	6.0581	(Charlier J.-B. et al, 2024)
FR-S-0021	France	Bief Poutot	47.0411	6.2507	(Charlier J.-B. et al, 2024)
GB-S-0001	UK	Blewbury	51.5672	-1.2388	Darling
					(Olarinoye et al., 2020)
GB-S-0002	UK	Letcombe_B	51.5652	-1.4608	Darling
					(Olarinoye et al., 2020)
GB-S-0003	UK	E_Ginge	51.5768	-1.3583	Darling

ID	Country	Name	Latitude	Longitude	References
GB-S-0004	UK	Jannaways	51.4252	-1.3546	Darling
GB-S-0005	UK	Kimber	51.4394	-1.1636	Darling
GB-S-0006	UK	Upton	51.5730	-1.2532	Darling
GB-S-0007	UK	Weston	51.4633	-1.4263	Darling
GB-S-0008	UK	Woolstone	51.5822	-1.5736	Darling
GR-S-0001	Greece	Uni Patras P1	37.8677	22.4733	Eleni Zagana
GR-S-0002	Greece	Uni Patras P2	37.8695	22.4640	Eleni Zagana
GR-S-0003	Greece	Meliggoi	39.5157	20.8149	(Katsanou, 2012; D'Alessandro et al., 2013)
GR-S-0004	Greece	Viros	39.4325	20.8403	(Katsanou, 2012; D'Alessandro et al., 2013)
GR-S-0005	Greece	Geroplatanos	39.3313	20.9445	(Katsanou, 2012; D'Alessandro et al., 2013)
GR-S-0006	Greece	Pesta	39.4600	20.9172	(Katsanou, 2012; D'Alessandro et al., 2013)
GR-S-0007	Greece	Sklivani	39.4327	20.9368	(Katsanou, 2012; D'Alessandro et al., 2013)
GR-S-0008	Greece	Priala	39.2346	20.8296	(Katsanou, 2012; D'Alessandro et al., 2013)
GR-S-0009	Greece	Agios Georgios	39.2702	20.8513	(Katsanou, 2012; D'Alessandro et al., 2013)
GR-S-0010	Greece	Skala	39.1757	20.7678	(Katsanou, 2012; D'Alessandro et al., 2013)
GR-S-0011	Greece	Kambi	39.2176	20.9020	(Katsanou, 2012; D'Alessandro et al., 2013)
GR-S-0012	Greece	Petra	39.1537	20.8220	(Katsanou, 2012; D'Alessandro et al., 2013)
GR-S-0013	Greece	Chanopoulo	39.1967	20.9404	(Katsanou, 2012; D'Alessandro et al., 2013)
HR-S-0001	Croatia	Rjecina Spring	45.4251	14.4242	(Mance et al., 2022)
HR-S-0002	Croatia	Perilo Spring	45.3072	14.535	(Mance et al., 2022)
HR-S-0003	Croatia	Dobra Spring	45.2992	14.5553	(Mance et al., 2022)
HR-S-0004	Croatia	Dobrica Spring	45.2964	14.5611	(Mance et al., 2022)

ID	Country	Name	Latitude	Longitude	References
HR-S-0005	Croatia	Krbavica main Spring	47.7190	15.6279	(Stroj et al., 2020)
HR-S-0006	Croatia	Zvir Spring	45.3344	14.4531	(Mance et al., 2022)
HR-S-0007	Croatia	Martinscica well 2	45.3181	14.48361	(Mance et al., 2022)
HU-S-0001	Hungary	Anyak	46.1363	18.2253	(Palcsu et al., 2021) (Fórizs et al., 2020)
HU-S-0002	Hungary	Csurgo	46.2030	18.3248	(Palcsu et al., 2021) (Fórizs et al., 2020)
HU-S-0003	Hungary	Pasztor	46.2183	18.3601	(Palcsu et al., 2021) (Fórizs et al., 2020)
IE-S-0001	Ireland	Kinvara (west)	53.1406	-8.9283	Laurence Gill / Ted McCormack)
IE-S-0002	Ireland	Kinvara (east)	53.1416	-8.9261	Laurence Gill / Ted McCormack)
IL-S-0001	Israel	Dan	33.2490	35.6530	Alon Rimmer / Heike Brielmann (Olarinoye et al., 2020)
IL-S-0002	Israel	Banias	33.2483	35.6946	Alon Rimmer / Heike Brielmann (Olarinoye et al., 2020)
IL-S-0003	Israel	Ein Harod	32.5480	35.3550	Lange (Olarinoye et al., 2020)
IL-S-0004	Israel	Ein Homa & Ein Migdal (close but different datasets in Wokas)	32.5000	35.4530	Lange (Olarinoye et al., 2020)
IL-S-0005	Israel	Ein Amall	32.5050	35.4450	Lange (Olarinoye et al., 2020)
IL-S-0006	Israel	Ein Moda	32.4960	35.4450	Lange (Olarinoye et al., 2020)
IL-S-0007	Israel	Leshem	33.2489	35.6514	Lange (Olarinoye et al., 2020)
IL-S-0008	Israel	Kezinim	33.2469	35.6878	Lange (Olarinoye et al., 2020)
IQ-S-0001	Iraq	Sarwchawa	36.2800	44.7573	(Mustafa et al., 2015)
IQ-S-0002	Iraq	Shkarta	36.3061	44.7219	(Mustafa et al., 2015)

ID	Country	Name	Latitude	Longitude	References
IQ-S-0003	Iraq	Betwata	36.3434	44.7088	(Mustafa et al., 2015)
IQ-S-0004	Iraq	Zewa	36.3956	44.6454	(Mustafa et al., 2015)
IQ-S-0005	Iraq	Chewqa	36.3490	44.5783	(Mustafa et al., 2015)
IQ-S-0006	Iraq	Bla	36.5186	44.4925	(Mustafa et al., 2015)
IQ-S-0007	Iraq	Qala Saida	36.3397	44.7647	(Mustafa et al., 2015)
IQ-S-0008	Iraq	Gullan	36.3881	44.6939	(Mustafa et al., 2015)
IT-S-0001	Italy	Molinetto	46.0079	12.4735	(Filippini et al., 2018)
IT-S-0002	Italy	Santissima	46.0210	12.4749	(Filippini et al., 2018)
IT-S-0003	Italy	Gorgazzo	46.0398	12.4969	(Filippini et al., 2018)
IT-S-0004	Italy	Pradidali Spring	46.2275	11.8689	(Lucianetti et al., 2019)
IT-S-0005	Italy	Agaroi	46.0703	12.5110	Maria Filippini /Stumpp
IT-S-0006	Italy	Budoia	46.0758	12.5117	Maria Filippini /Stumpp
IT-S-0007	Italy	Tornidor	46.0729	12.5106	Maria Filippini /Stumpp
IT-S-0008	Italy	Polla1 Santissima	46.0177	12.4762	Maria Filippini /Stumpp
IT-S-0009	Italy	Polla2 Santissima	46.0180	12.4764	Maria Filippini /Stumpp
IT-S-0010	Italy	Cavalli	46.0098	12.4772	Maria Filippini /Stumpp
IT-S-0011	Italy	Angheraz Spring	46.2839	11.9218	Ente Parco di Paneveggio Pale di San Martino
IT-S-0012	Italy	Poiano Spring	44.3875	10.4375	(Ronchetti et al., 2023)
IT-S-0013	Italy	Capodacqua di Spigno Spring	41.2857	13.7149	(Iacurto et al., 2021)
IT-S-0014	Italy	Mazzoccolo Spring	41.2593	13.6080	Giuseppe Sappa /Silvia Iacurto
IT-S-0015	Italy	S1 (Longano)	41.5167	14.2498	(Aquino et al., 2015) (Centro Funzionale Multirischi di Protezione Civile Regione Campania, 2025)
IT-S-0016	Italy	La Marca Spring	41.9143	13.8781	(Petitta et al., 2010)
IT-S-0017	Italy	Pila Spring	41.1449	14.2615	(Corniello et al., 2024) (Centro Funzionale Multirischi di Protezione Civile Regione Campania, 2025)
IT-S-0018	Italy	Triflisco Spring	41.1361	14.2542	(Corniello et al., 2024)

ID	Country	Name	Latitude	Longitude	References
					(Centro Funzionale Multirischi di Protezione Civile Regione Campania, 2025)
IT-S-0019	Italy	S.Sofia Spring	41.1409	14.3248	(Corniello et al., 2024) (Centro Funzionale Multirischi di Protezione Civile Regione Campania, 2025)
JO-S-0001	Jordan	Tanour Spring	32.4080	35.7450	(Hamdan et al., 2016)
KO-S-0001	Korea	S41 Spring	37.2361	128.4894	(Yu et al., 2021)
KO-S-0002	Korea	S45 Spring	37.2361	128.4894	(Yu et al., 2021)
KO-S-0003	Korea	S46 Spring	37.2361	128.4894	(Yu et al., 2021)
LB-S-0001	Lebanon	Jeita	33.9436	35.6420	(Margne and Stoeckl, 2013) (Königer and Margane, 2014)
LB-S-0002	Lebanon	Naber al Labbane	33.9947	35.8284	(Margne and Stoeckl, 2013) (Königer and Margane, 2014)
LB-S-0003	Lebanon	Naber al Assal	34.0099	35.8385	(Margne and Stoeckl, 2013) (Königer and Margane, 2014)
LB-S-0004	Lebanon	Kashkoush	33.9428	35.6390	(Margne and Stoeckl, 2013) (Königer and Margane, 2014)
LB-S-0005	Lebanon	Afqa	34.0678	35.8933	(Margne and Stoeckl, 2013) (Königer and Margane, 2014)
LB-S-0006	Lebanon	Rouaiss	34.1089	35.9090	(Margne and Stoeckl, 2013) (Königer and Margane, 2014)
MA-S-0001	Morocco	WT Spring	30.6806	-9.3448	Applied Geology and Geo-Environment Laboratory, Ibn Zohr University
PA-S-0001	Panama	Sultan_Elisha	31.8697	35.4433	(Kroitoru et al., 1985; Schmidt, 2014)
PA-S-0002	Panama	Fara	31.8333	35.2991	(Kroitoru et al., 1985)
SI-S-0001	Slovenia	Timavo	45.7863	13.5873	(Doctor and Alexander, 2005)
SI-S-0002	Slovenia	Sardos	45.7929	13.5866	(Doctor and Alexander, 2005)
SI-S-0003	Slovenia	Moschenizze_North	45.8030	13.5817	(Doctor and Alexander, 2005)
SK-S-0001	Slovakia	Drienovec Spring	48.6249	20.9523	Alena Gessert

ID	Country	Name	Latitude	Longitude	References
SK-S-0002	Slovakia	Vinica	48.6227	20.8914	Alena Gessert
SK-S-0003	Slovakia	Pekna Dievcina	48.6742	20.9762	Alena Gessert
SK-S-0004	Slovakia	Teplica	48.6749	20.9458	Alena Gessert
SK-S-0005	Slovakia	Sv. Jan	48.6538	20.9747	Alena Gessert
SK-S-0006	Slovakia	Kozia Studna	48.6438	20.8695	Alena Gessert
SK-S-0007	Slovakia	Skalisty	48.6226	20.8914	(Palcsu et al., 2021)
UA-S-0001	Ukraine	Skelsky Spring	44.4333	33.9000	(Dublyansky et al., 2018, 2019)
UA-S-0002	Ukraine	Ogni Grifona Spring	44.4500	33.8667	(Dublyansky et al., 2018, 2019)
UA-S-0003	Ukraine	Mikhailovsky Spring	45.3453	34.4997	(Dublyansky et al., 2019)
UA-S-0004	Ukraine	Panija Spring	45.3453	34.4997	(Dublyansky et al., 2019)
UA-S-0005	Ukraine	Boldyrevsky Spring	45.3453	34.4997	(Dublyansky et al., 2019)
US-S-0001	USA	Clover Spring	34.5059	-110.3627	(Donovan et al., 2021, 2022)
US-S-0002	USA	Hoxworth Spring	35.0403	-111.4750	(Donovan et al., 2021, 2022)
US-S-0003	USA	Robber's Roost Spring	36.2805	-112.0889	(Donovan et al., 2021, 2022)
US-S-0004	USA	North Canyon Spring	36.3975	-112.0846	(Donovan et al., 2021, 2022)
US-S-0005	USA	BS1 Spring	29.8294	-98.8644	(Tian et al., 2021a)
US-S-0006	USA	BS2 Spring	29.8344	-98.8614	(Tian et al., 2021a)
US-S-0007	USA	Blue Hole Spring	29.4689	-98.4675	(Tian et al., 2021a)
US-S-0008	USA	San Pedro Spring	29.4469	-98.5017	(Tian et al., 2021a)
US-S-0009	USA	Comal Spring	29.7089	-98.1353	(Tian et al., 2021a)
					(USGS Water Data for the Nation, 2025)
US-S-0010	USA	Sulphur Springs	28.0211	-82.4516	(Zengin, 2022)
					(USGS Water Data for the Nation, 2025)
US-S-0011	USA	Tippery Spring	40.5689	-78.1560	(Berglund, 2019)
US-S-0012	USA	Near Tippery Spring	40.5685	-78.1558	(Berglund, 2019)
US-S-0013	USA	Royal Spring	38.2094	-84.5619	(Husic et al., 2019)
US-S-0014	USA	Rockwoods Spring	38.5683	-90.6664	(Criss et al., 2001)
US-S-0015	USA	Weldon Spring	37.71319	-90.68759	(Criss et al., 2001)
US-S-0016	USA	Natural Bridge Spring	30.2851	-84.1473	(Ahmed et al., 2021)
US-S-0017	USA	Orangeville Rise Spring	38.6303	-86.5572	(Burgess et al., 2021)

ID	Country	Name	Latitude	Longitude	References
US-S-0018	USA	Trout Farm Spring	33.5925	-105.5836	(Hoy, 1982; Mcada, 1993)
US-S-0019	USA	Cleve's Spring	32.9494	-105.2822	(Hoy, 1982; Mcada, 1993)
US-S-0020	USA	Paul Spring	32.9325	-105.2800	(Hoy, 1982; Mcada, 1993)
US-S-0021	USA	Boiling Spring	32.5592	-104.3903	(Hoy, 1982; Mcada, 1993)
US-S-0022	USA	Macho Spring	33.7081	-105.4031	(Hoy, 1982; Mcada, 1993)

Table S2: Cave sites included in the WoKaS-Iso database

ID	Country	Name	Latitude	Longitude	References
AT-C-0001	Austria	Obir Cave	46.5094	14.5483	(Spötl et al., 2005)
AT-C-0002	Austria	Katerloch Cave	47.0833	15.5500	(Boch et al., 2008) (Boch et al., 2011)
AT-C-0003	Austria	HGH Cave	47.6016	15.0930	NaN
AU-C-0001	Australia	Cathedral Cave	-32.6215	148.9400	(Cuthbert et al., 2014)
AU-C-0002	Australia	Golgotha Cave	-34.0830	115.0500	(Treble et al., 2013, 2015, 2022) (Griffiths et al., 2022)
AU-C-0003	Australia	Harrie Wood Cave	-35.7000	148.5000	(Tadros et al., 2016, 2022)
AU-C-0004	Australia	Little Trimmer Cave	-41.5667	146.2500	(Geode and Harmon, 1982)
AU-C-0005	Australia	Frankcombe Cave	-42.5333	146.4500	(Geode and Harmon, 1982)
AU-C-0006	Australia	Wombeyan Caves	-34.3086	149.9667	(Bian et al., 2019)
AU-C-0007	Australia	South Glory Cave	-35.7248	148.4875	(Coleborn et al., 2016, 2018, 2019) (Tadros et al., 2016)
AU-C-0008	Australia	Yonderup Cave	-31.5470	115.6900	(Nagra et al., 2016)
BR-C-0001	Brazil	Santana Cave	-24.5308	-48.7267	(Cruz et al., 2005)
BZ-C-0001	Belize	Yok Balum Cave	16.2086	-89.0735	(Ridley et al., n.d.)
CN-C-0001	China	Xianren Cave	24.1310	104.1333	(Duan et al., 2016)
CN-C-0002	China	Baojinggong Cave	24.1200	113.3500	(Duan et al., 2016)
CN-C-0003	China	Liangfeng Cave	26.2670	108.0500	(Duan et al., 2016)
CN-C-0004	China	Furong Cave	29.2289	107.9036	(Duan et al., 2016)
CN-C-0005	China	Penglaixian Cave	30.2333	117.5333	(Duan et al., 2016)
CN-C-0006	China	Heshang Cave	30.4500	110.4167	(Duan et al., 2016)
CN-C-0007	China	Wanxiang Cave	33.3200	105.0000	(Duan et al., 2016)
CN-C-0008	China	Shihua Cave	39.7833	115.9333	(Duan et al., 2016)
CN-C-0009	China	Yongxing Cave	31.5833	111.2333	(Wang et al., 2018)

ID	Country	Name	Latitude	Longitude	References
CN-C-0010	China	Maomaotuo Big Cave	25.3000	110.2667	(Yin et al., 2020)
CN-C-0011	China	Jiguan Cave	33.7667	111.5667	(Chen et al., 2023)
CN-C-0012	China	Yuhua Cave	26.8333	117.4333	(Qiu et al., 2023)
CN-C-0013	China	Zhenzhu cave	38.2500	113.7000	(Li et al., 2019)
CN-C-0014	China	Shenong Cave	28.7000	117.2500	(Tian et al., 2021b)
CN-C-0015	China	Shenqi Cave	28.9333	103.1000	(Zhao et al., 2022)
CN-C-0016	China	Yangkou Cave	29.0300	107.1800	(Chen and Li, 2018)
CZ-C-0001	Czech Republic	Byci Skala Cave	49.3087	16.6985	NaN
CZ-C-0002	Czech Republic	Punkva Caves	49.3722	16.7271	NaN
CZ-C-0003	Czech Republic	Katerinska Cave	49.3617	16.7125	NaN
CZ-C-0004	Czech Republic	Amaterska Cave	49.3842	16.7379	NaN
DE-C-0001	Germany	Bunker Cave	51.3675	7.6647	(Riechelmann et al., 2011, 2013, 2017)
ES-C-0001	Spain	Molinos Cave	40.7925	-0.4492	(Moreno et al., 2014)
ES-C-0002	Spain	La Vina cave	42.1793	-2.7010	(Osácar et al., 2014)
ES-C-0003	Spain	La Paz cave	42.1793	-2.7010	(Osácar et al., 2014)
ES-C-0004	Spain	Ejulve Cave	40.7600	-0.5900	(Pérez-Mejías et al., 2018)
ES-C-0005	Spain	Cueva de Asiul	43.3200	-3.5900	(Smith et al., 2015)
ES-C-0006	Spain	La Garma Cave	43.4306	-3.6658	(Baldini et al., 2015)
ES-C-0007	Spain	Mendukilo Cave	42.9736	-1.8958	(Bernal-Wormull et al., 2023)
FR-C-0002	France	Grotte de Villars	45.4300	0.7800	(Genty et al., 2014)
FR-C-0003	France	Chauvet Cave	44.3875	4.4165	(Genty et al., 2014)
GB-C-0001	UK	Uamh an Tartair	58.1400	-4.9300	(Fuller et al., 2007, 2008)
GT-C-0001	Guatemala	Gruta del Rey Marcos	15.4244	-90.3283	(Bernal et al., 2023)
GU-C-0001	Guam	Jinapsan Cave	13.6333	144.8833	(Partin et al., 2012)
HR-C-0001	Croatia	Nova Grgosova Cave	45.8188	15.6783	(Surić et al., 2018)
HR-C-0002	Croatia	Lokvarka Cave	45.8167	15.6667	(Surić et al., 2018)
HR-C-0003	Croatia	Lower Barac Cave	44.9833	15.7167	(Czuppon et al., 2017)
HR-C-0004	Croatia	Upper Barac Cave	44.9844	15.7217	(Czuppon et al., 2017)
HR-C-0005	Croatia	Modric Cave	44.2568	15.5372	(Surić et al., 2018)
HR-C-0006	Croatia	Strasna Pec Cave	44.0000	15.0333	(Surić et al., 2017)
HR-C-0007	Croatia	Manita Pec Cave	44.3000	15.4667	(Surić et al., 2017)

ID	Country	Name	Latitude	Longitude	References
HR-C-0008	Croatia	Spilja U Zubu Buljme Cave	44.3656	15.4661	(Surić et al., 2017)
HU-C-0001	Hungary	Beke Cave	48.4833	20.5167	(Czuppon et al., 2017)
IN-C-0001	India	Dharamjali Cave	29.5247	80.2078	(Giesche, A et al. 2023)
IN-C-0002	India	Mawmluh Cave India	25.2622	91.8817	(Breitenbach et al., 2015)
IN-C-0003	India	Akalagavi cave	14.9833	74.5167	(Kaushal, 2017)
MX-C-0001	Mexico	Rio Secreto Cave	20.5900	-87.1300	(Lases-Hernández et al., 2020)
MY-C-0001	Malaysia	Wind Cave	4.0333	114.8000	(Moerman et al., 2013) (Ellis et al., 2020)
NZ-C-0001	New Zealand	Aranui Cave	-38.2662	175.0767	(Williams and Fowler, 2002)
NZ-C-0002	New Zealand	Waipuna Cave	-38.3115	175.0206	(Nava-Fernandez et al., 2020)
PR-C-0001	Puerto Rico	Larga Cave	18.3200	-66.8000	(Vieten et al., 2018b, a) (Warken et al., 2022)
RO-C-0001	Romania	Ascunsa Cave	45.0000	22.6000	(Dragusin et al., 2017) (IAEA, 2025)
RO-C-0002	Romania	Closani Cave	45.1000	22.8000	(Warken et al., 2018)
SI-C-0001	Slovenia	Postojna Cave	45.7700	14.2000	(Domínguez-Villar et al., 2018)
US-C-0001	USA	West Cave	30.3394	-98.1408	(Feng et al., 2014)
US-C-0002	USA	Inner Space Cavern	30.6080	-97.6881	(Pape et al., 2010)
US-C-0003	USA	Caverns of Sonora	30.5500	-100.8167	(Pape et al., 2010)
US-C-0004	USA	Natural Bridge Cavern	29.6900	-98.3400	(Pape et al., 2010)
US-C-0005	USA	DeSoto Caverns	33.3072	-86.2767	(Joe Lambert and Aharon, 2010)
US-C-0006	USA	Indian Oven Cave	41.9000	-73.5000	(van Beynen and Febbroriello, 2006)
US-C-0007	USA	Carlsbad Caverns	32.1479	-104.5667	(Chapman et al., 1986, 1992) (Hoy et al., 1982) (Turin et al., 2022)
US-C-0008	USA	Cave Without A Name	29.8852	-98.6208	(Miller et al., 2021) (Pape et al., 2010)

References

Ahmed, N., Ye, M., Wang, Y., Greenhalgh, T., and Fowler, K.: Using δ18O and δ2H to Detect Hydraulic Connection Between a Sinkhole Lake and a First-Magnitude Spring, Groundwater, 59, 856–865, https://doi.org/10.1111/GWAT.13105, 2021.

Antonio, J. and Fornell, B.: Preparatory actions for the development and implementation of Early Warning Systems (EWS) for spring water contamination, Open File Rep., 2020.

Aquilina, L., Ladouche, B., and Dörfliger, N.: Water storage and transfer in the epikarst of karstic systems during high flow periods, J Hydrol (Amst), 327, 472–485, https://doi.org/10.1016/j.jhydrol.2005.11.054, 2006.

Aquino, D., Petrella, E., Florio, M., Celico, P., and Celico, F.: Complex hydraulic interactions between compartmentalized carbonate aquifers and heterogeneous siliciclastic successions: A case study in southern Italy, Hydrol Process, 29, 4252–4263, https://doi.org/10.1002/HYP.10499, 2015.

Baldini, L. M., McDermott, F., Baldini, J. U. L., Arias, P., Cueto, M., Fairchild, I. J., Hoffmann, D. L., Mattey, D. P., Müller, W., Nita, D. C., Ontañón, R., Garciá-Moncó, C., and Richards, D. A.: Regional temperature, atmospheric circulation, and sea-ice variability within the Younger Dryas Event constrained using a speleothem from northern Iberia, Earth Planet Sci Lett, 419, 101–110, https://doi.org/10.1016/J.EPSL.2015.03.015, 2015.

Barberá-Fornell, J. A.: Investigaciones hidrogeológicas en los acuíferos carbonáticos de la Serranía Oriental de Ronda (Málaga), Ph.D. thesis, Universidad de Málaga, España, 2014.

Berglund, J. L.: Karst aquifer recharge and conduit flow dynamics from high-resolution monitoring and transport modeling in gentral pennsylvania springs, Ph.D. thesis, Temple University, USA, https://doi.org/10.34944/DSPACE/2578, 2019.

Bernal, J. P., Revolorio, F., Cu-Xi, M., Lases-Hernández, F., Piacsek, P., Lachniet, M. S., Beddows, P. A., Lucia, G., López-Aguiar, K., Capella-Vizcaíno, S., López-Martínez, R., and Vásquez, O. J.: Variability of trace-elements and δ18O in drip water from Gruta del Rey Marcos, Guatemala; seasonal and environmental effects, and its implications for paleoclimate reconstructions, Front Earth Sci (Lausanne), 11, 1112957, https://doi.org/10.3389/FEART.2023.1112957, 2023.

Bernal-Wormull, J. L., Moreno, A., Bartolomé, M., Arriolabengoa, M., Pérez-Mejías, C., Iriarte, E., Osácar, C., Spötl, C., Stoll, H., Cacho, I., Edwards, R. L., and Cheng, H.: New insights into the climate of northern Iberia during the Younger Dryas and Holocene: The Mendukilo multi-speleothem record, Quat Sci Rev, 305, 108006, https://doi.org/10.1016/J.QUASCIREV.2023.108006, 2023.

van Beynen, P. and Febbroriello, P.: Seasonal isotopic variability of precipitation and cave drip water at Indian Oven Cave, New York, Hydrol Process, 20, 1793–1803, https://doi.org/10.1002/HYP.5957, 2006.

Bian, F., Coleborn, K., Flemons, I., Baker, A., Treble, P. C., Hughes, C. E., Baker, A., Andersen, M. S., Tozer, M. G., Duan, W., Fogwill, C. J., and Fairchild, I. J.: Hydrological and geochemical responses of fire in a shallow cave system, Science of The Total Environment, 662, 180–191, https://doi.org/10.1016/J.SCITOTENV.2019.01.102, 2019.

Boch, R., Mag, U., and Spötl, C.: Stalagmites from Katerloch Cave, Austria: Growth dynamics and high-resolution records of climate change, Ph.D. thesis, Austria, 2008.

Boch, R., Spötl, C., and Frisia, S.: Origin and palaeoenvironmental significance of lamination in stalagmites from Katerloch Cave, Austria, Sedimentology, 58, 508–531, https://doi.org/10.1111/j.1365-3091.2010.01173.x, 2011.

Breitenbach, S. F. M., Lechleitner, F. A., Meyer, H., Diengdoh, G., Mattey, D., and Marwan, N.: Cave ventilation and rainfall signals in dripwater in a monsoonal setting – a monitoring study from NE India, Chem Geol, 402, 111–124, https://doi.org/10.1016/J.CHEMGEO.2015.03.011, 2015.

Burgess, S. A., Florea, L., and Branam, T. D.: Sulfur systematics and carbonate diagenesis in the Mitchell plateau, Indiana, in: GSA connects 2021, Portland, Oregon, 2021.

Centro Funzionale Multirischi di Protezione Civile Regione Campania: Civile Regione Campania data portal, available at: https://centrofunzionale.regione.campania.it/home#/pages/dashboard, last access: 21 December 2025.

Chapman, J. B.: Stable isotopes in southeastern New Mexico groundwater: implications for dating recharge in the WIPP area. State of New Mexico Environmental Evaluation Group, Santa Fe, NM, Rep. EEG-35, 76 pp, 1986.

Chapman, J. B., Ingraham, N. L., and Hess, J. W.: Isotopic investigation of infiltration and unsaturated zone flow processes at Carlsbad Cavern, New Mexico, J Hydrol (Amst), 133, 343–363, https://doi.org/10.1016/0022-1694(92)90262-T, 1992.

Charlier J.-B.: NUTRI-Karst – Echanges karst-rivière et fonctionnement hydrogéologique des aquifères du bassin de la Loue. BRGM/RP-73496-FR report, 261 p, 2024.

Chen, C. J. and Li, T. Y.: Geochemical characteristics of cave drip water respond to ENSO based on a 6-year monitoring work in Yangkou Cave, Southwest China, J Hydrol (Amst), 561, 896–907, https://doi.org/10.1016/J.JHYDROL.2018.04.061, 2018.

Chen, X., Jiang, X., Wang, X., Zhao, J., Sun, Z., Li, Y., Ye, Z., Cai, J., Fu, X., Xu, Y., and Yang, Y.: New insights into potential effects of solar activity on the oxygen isotope composition of modern speleothems: Observations from Jiguan Cave, central China II, J Hydrol (Amst), 625, 130114, https://doi.org/10.1016/J.JHYDROL.2023.130114, 2023.

Coleborn, K., Rau, G. C., Cuthbert, M. O., Baker, A., and Navarre, O.: Solar-forced diurnal regulation of cave drip rates via phreatophyte evapotranspiration, Hydrol. Earth Syst. Sci, 20, 4439–4455, https://doi.org/10.5194/hess-20-4439-2016, 2016.

Coleborn, K., Baker, A., Treble, P. C., Andersen, M. S., Baker, A., Tadros, C. V., Tozer, M., Fairchild, I. J., Spate, A., and Meehan, S.: The impact of fire on the geochemistry of speleothem-forming drip water in a sub-alpine cave, Sci Total Environ, 642, 408–420, https://doi.org/10.1016/J.SCITOTENV.2018.05.310, 2018.

Coleborn, K., Baker, A., Treble, P. C., Andersen, M. S., Baker, A., Tadros, C. V., Tozer, M., Fairchild, I. J., Spate, A., and Meehan, S.: Corrigendum to "The impact of fire on the geochemistry of speleothem-forming drip water in a sub-alpine cave" [Sci. Total Environ. (2018) 408–420], Science of The Total Environment, 668, 1339–1340, https://doi.org/10.1016/J.SCITOTENV.2019.02.350, 2019.

Corniello, A., Ducci, D., Stellato, L., Stevenazzi, S., Massaro, L., and Del Gaudio, E.: Combining groundwater budget, hydrochemistry and environmental isotopes to identify the groundwater flow in carbonate aquifers located in Campania Region (Southern Italy), J Hydrol Reg Stud, 53, 101790, https://doi.org/10.1016/J.EJRH.2024.101790, 2024.

Criss, R. E., Fernandes, S. A., and Winston, W. E.: Isotopic, Geochemical and Biological Tracing of the Source of an Impacted Karst Spring, Weldon Spring, Missouri, Environ Forensics, 2, 99–103, https://doi.org/10.1006/ENFO.2000.0034, 2001.

Cruz, F. W., Karmann, I., Viana, O., Burns, S. J., Ferrari, J. A., Vuille, M., Sial, A. N., and Moreira, M. Z.: Stable isotope study of cave percolation waters in subtropical Brazil: Implications for paleoclimate inferences from speleothems, Chem Geol, 220, 245–262, https://doi.org/10.1016/J.CHEMGEO.2005.04.001, 2005.

Cuthbert, M. O., Baker, A., Jex, C. N., Graham, P. W., Treble, P. C., Andersen, M. S., and Ian Acworth, R.: Drip water isotopes in semi-arid karst: Implications for speleothem paleoclimatology, Earth Planet Sci Lett, 395, 194–204, https://doi.org/10.1016/J.EPSL.2014.03.034, 2014.

Czuppon, G., Demény, A., Leél-Őssy, S., Óvari, M., Molnár, M., Stieber, J., Kiss, K., Kármán, K., Surányi, G., and Haszpra, L.: Cave monitoring in the Béke and Baradla caves (Northeastern Hungary): implications for the conditions for the formation cave carbonates, International Journal of Speleology, 47: 13-28, https://doi.org/10.5038/1827-806X.47.1.2110, 2017

D'Alessandro, W., Katsanou, K., Lambrakis, N., Bellomo, S., Brusca, L., and Liotta, M.: Chemical and isotopic characterisation of bulk deposition in the Louros basin (Epirus, Greece), Atmos Res, 132–133, 399–410, https://doi.org/10.1016/J.ATMOSRES.2013.07.007, 2013.

Doctor, D. H. and Alexander, E. C.: Interpretation of Water Chemistry and Stable Isotope Data from a Karst Aquifer According to Flow Regimes Identified through Hydrograph Recession Analysis, 2005.

Domínguez-Villar, D., Lojen, S., Krklec, K., Kozdon, R., Edwards, R. L., and Cheng, H.: Ion microprobe δ18O analyses to calibrate slow growth rate speleothem records with regional δ18O records of precipitation, Earth Planet Sci Lett, 482, 367–376, https://doi.org/10.1016/J.EPSL.2017.11.012, 2018.

Donovan, K.M: Karst Spring Processes and Storage Implications in High Elevation, Semiarid Southwestern United States, Master thesis, Northern Arizona University, USA, 2021.

Donovan, K.M., Springer, A.E., Tobin, B.W. and Parnell, R.A.: Karst Spring Processes and Storage Implications in High Elevation, Semiarid Southwestern United States. In Threats to Springs in a Changing World (eds M.J. Currell and B.G. Katz). https://doi.org/10.1002/9781119818625.ch4, 2022.

Dragusin, V., Balan, S., Blamart, D., Lázár Forray, F., Marin, C., Mirea, I., Nagavciuc, V., Oraseanu, I., Peraoiu, A., Tia, L., Tudorache, A., and Vlaicu, M.: Transfer of environmental signals from the surface to the underground at Ascunsa Cave, Romania, Hydrol Earth Syst Sci, 21, 5357–5373, https://doi.org/10.5194/HESS-21-5357-2017, 2017.

Duan, W., Ruan, J., Luo, W., Li, T., Tian, L., Zeng, G., Zhang, D., Bai, Y., Li, J., Tao, T., Zhang, P., Baker, A., and Tan, M.: The transfer of seasonal isotopic variability between precipitation and drip water at eight caves in the monsoon regions of China, Geochim Cosmochim Acta, 183, 250–266, https://doi.org/10.1016/j.gca.2016.03.037, 2016.

Dublyansky, Y. V., Klimchouk, A. B., Tokarev, S. V., Amelichev, G. N., Langhamer, L., and Spötl, C.: Stable isotopic composition of atmospheric precipitation on the Crimean Peninsula and its controlling factors, J Hydrol (Amst), 565, 61–73, https://doi.org/10.1016/J.JHYDROL.2018.08.006, 2018.

Dublyansky, Y. V., Klimchouk, A. B., Tokarev, S. V., Amelichev, G. N., and Spötl, C.: Groundwater of the Crimean Peninsula: a first systematic study using stable isotopes, Isotopes Environ Health Stud, 55, 419–437, https://doi.org/10.1080/10256016.2019.1650743, 2019.

eHYD – access to Austria's hydrographic data: https://ehyd.gv.at/, last access: 14 April 2025.

Ellis, S. A., Cobb, K. M., Moerman, J. W., Partin, J. W., Bennett, A. L., Malang, J., Gerstner, H., and Tuen, A. A.: Extended Cave Drip Water Time Series Captures the 2015–2016 El Niño in Northern Borneo, Geophys Res Lett, 47, no-no, https://doi.org/10.1029/2019GL086363, 2020.

Feng, W., Casteel, R. C., Banner, J. L., and Heinze-Fry, A.: Oxygen isotope variations in rainfall, drip-water and speleothem calcite from a well-ventilated cave in Texas, USA: Assessing a new speleothem temperature proxy, Geochim Cosmochim Acta, 127, 233–250, https://doi.org/10.1016/J.GCA.2013.11.039, 2014.

Filippini, M., Squarzoni, G., De Waele, J., Fiorucci, A., Vigna, B., Grillo, B., Riva, A., Rossetti, S., Zini, L., Casagrande, G., Stumpp, C., and Gargini, A.: Differentiated spring behavior under changing hydrological conditions in an alpine karst aquifer, J Hydrol (Amst), 556, 572–584, https://doi.org/10.1016/J.JHYDROL.2017.11.040, 2018.

Fórizs, I., Kern, Z., Csicsák, J., Csurgó, G., Földing, G., Máthé, Z., Ország, J., Szreda, G., and Vendégh, R.: Monthly data of stable isotopic composition (δ18O, δ2H) and tritium activity in precipitation from 2004 to 2017 in the Mecsek Hills, Hungary, Data Brief, 32, 106206, https://doi.org/10.1016/J.DIB.2020.106206, 2020.

Fuller, L.: High-resolution multiproxy geochemical Holocene climate records from 1000-year-old Scottish stalagmites, Unpublished PhD thesis, University of Birmingham, Birmingham, UK, 2007.

Fuller, L., Baker, A., Fairchild, I. J., Spötl, C., Marca-Bell, A., Rowe, P., and Dennis, P. F.: Isotope hydrology of drip waters in a Scottish cave and implications for stalagmite palaeoclimate research, Hydrol Earth Syst Sci, 12, 1065–1074, https://doi.org/10.5194/HESS-12-1065-2008, 2008.

Genty, D., Labuhn, I., Hoffmann, G., Danis, P. A., Mestre, O., Bourges, F., Wainer, K., Massault, M., Van Exter, S., Régnier, E., Orengo, P., Falourd, S., and Minster, B.: Rainfall and cave water isotopic relationships in two South-France sites, Geochim Cosmochim Acta, 131, 323–343, https://doi.org/10.1016/J.GCA.2014.01.043, 2014.

Geode, A. and Harmon, R. S.: Isotopic composition of precipitation, cave drips and activity forming speleothems at three Tasmanian cave sites, Helictite journal, 1982.

Giesche, A., Hodell, D. A., Petrie, C. A., Haug, G. H., Adkins, J. F., Plessen, B., Marwan, N., Bradbury, H. J., Hartland, A., French, A. D., Breitenbach, S. F. M.: Cave measurements made during the field campaign in April and October 2006, including δD and $\delta^{18}O$ from cave drip water, a nearby pond, and rainwater (Table X4) [dataset]. PANGAEA, https://doi.org/10.1594/PANGAEA.956777, 2023.

Griffiths, A. D., Treble, P. C., Hope, P., Rudeva, I., Griffiths, A. D., Treble, P. C., Hope, P., and Rudeva, I.: Rainfall Stable Water Isotope Variability in Coastal Southwestern Western Australia and Its Relationship to Climate on Multiple Timescales, JGRD, 127, e2021JD035433, https://doi.org/10.1029/2021JD035433, 2022.

Guo, X., Chen, Q., Huang, H., Wang, Z., Li, J., Huang, K., and Zhou, H.: Water source identification and circulation characteristics of intermittent karst spring based on hydrochemistry and stable isotope—An example from Southern China, Applied Geochemistry, 141, 105309, https://doi.org/10.1016/J.APGEOCHEM.2022.105309, 2022.

Guo, Y., Qin, D., Li, L., Sun, J., Li, F., and Huang, J.: A complicated karst spring system: identified by karst springs using water level, Hydrogeochemical, and Isotopic Data in Jinan, China, Water 2019, Vol. 11, Page 947, 11, 947, https://doi.org/10.3390/W11050947, 2019.

Hamdan, I., Wiegand, B., Toll, M., and Sauter, M.: Spring response to precipitation events using $\delta^{18}O$ and $\delta^{2}H$ in the Tanour catchment, NW Jordan, Isotopes Environ Health Stud, 52, 682–693, https://doi.org/10.1080/10256016.2016.1159205, 2016.

Hoy, R. N.: Baseline study of Oxygen 18 and deuterium in the Roswell, New Mexico, groundwater basin, 1982.

Huang, H. And Liu, H.: The hydrogen and oxygen stable isotope analysis of the karst spring in Heilongtan, *CARSOLOGICA SINICA*, 2015, 34(5): 445-451, https://doi.org/10.11932/karst20150504, 2015.

Humer, F., Brielmann, H., Kralik, M., and Wemhöner, U.: Grundwasseralter von ausgewählten Grundwasserkörpern (GW-Alter 2014–15) – Böhmische Masse [MAR], Hügelland zwischen Mur und Raab, Lafnitztal, Mittleres Ennstal, Stooberbachtal, Weststeirisches Hügelland, Zentralzone (Tiroler Anteil). Endbericht 2015, Wien, 2015.

Husic, A., Fox, J., Adams, E., Backus, J., Pollock, E., Ford, W., and Agouridis, C.: Inland impacts of atmospheric river and tropical cyclone extremes on nitrate transport and stable isotope measurements. Environ Earth Sci 78, 36, https://doi.org/10.1007/s12665-018-8018-x, 2019.

Iacurto, S., Grelle, G., De Filippi, F. M., and Sappa, G.: Karst recharge areas identified by combined application of isotopes and hydrogeological budget, Water 2021, Vol. 13, Page 1965, 13, 1965, https://doi.org/10.3390/W13141965, 2021.

International Atomic Energy Agency (IAEA): WISER – Water Isotope System for Data Analysis, Visualization and Electronic Retrieval, available at: https://nucleus.iaea.org/wiser, last access: 14 April 2025.

Joanneum Research, Fachhochschule Technikum Wien, Wasser Tirol Wasserdienstleisungs-GesmbH, Illwerke-Wassermanagement GmbH, W.E.I.Z. Weizer Energie-Innovations-Zentrum GmbH, Logotronic GmbH, and Hereschwerke Automation GmbH: KNet Endbericht, Netzknote, 2008.

Joe Lambert, W. and Aharon, P.: Oxygen and hydrogen isotopes of rainfall and drip water at DeSoto Caverns (Alabama, USA): Key to understanding past variability of moisture transport from the Gulf of Mexico, Geochim Cosmochim Acta, 74, 846–861, https://doi.org/10.1016/J.GCA.2009.10.043, 2010.

Katsanou, K.: Environmental hydrogeological study of Louros watershed, Ph.D. thesis, University of Patras, Greece, 2012.

Kaushal, N.: High resolution paleo-monsoon records from peninsular Indian speleothems, Ph.D. thesis, University of Oxford, UK, 2017.

Königer, P. and Margane, A.: German-Lebanese Technical Cooperation Project Protection of Jeita Spring Stable Isotope Investigations in the Jeita Spring catchment, 2014.

Kralik, M.: Verweilzeiten Vorarlberger Brunnen und Quellen 2014; als Grundlage für die Errichtung einer Notwasserversorgung, Unpublished report, Bregenz, 20 pp., 2015.

Kroitoru, L., Mazor, E., and Gilad, D.: Hydrological characteristics of the Wadi Kelt and Elisha springs, IAHS-AISH publication, 1985.

Lases-Hernández, F., Medina-Elizalde, M., and Benoit Frappier, A.: Drip water δ18O variability in the northeastern Yucatán Peninsula, Mexico: Implications for tropical cyclone detection and rainfall reconstruction from speleothems, Geochim Cosmochim Acta, 285, 237–256, https://doi.org/10.1016/J.GCA.2020.07.008, 2020.

Li, Y., Zhang, S., Liu, X., Gao, Y., and Rao, Z.: Variations of the stable isotopic composition of precipitation and cave drip water at zhenzhu cave, north China: a two-year monitoring study, Journal of Cave and Karst Studies, 81, 123–135, https://doi.org/10.4311/2018ES0128, 2019.

Lucianetti, G., Mastrorillo, L., Mazza, R., and Partel, P.: Groundwater response to precipitation extremes: The case of the “Vaia” storm (Eastern Italian Alps), Acque Sotterranee - Italian Journal of Groundwater, 8, 39–45, https://doi.org/10.7343/AS-2019-429, 2019.

Luo, M., Chen, Z., Criss, R. E., Zhou, H., Huang, H., Han, Z., and Shi, T.: Dynamics and anthropogenic impacts of multiple karst flow systems in a mountainous area of South China. Hydrogeol J 24, 1993–2002, https://doi.org/10.1007/s10040-016-1462-3, 2016.

Luo, M., Chen, Z., Zhou, H., Zhang, L., and Han, Z.: Hydrological response and thermal effect of karst springs linked to aquifer geometry and recharge processes. Hydrogeol J 26, 629–639, https://doi.org/10.1007/s10040-017-1664-3, 2018.

Lyu, L., Li, W., Liu, Y., Song, M., Deng, Q., and Zheng, Y.: Dynamic analysis of hydrochemistry and isotope of the karst spring of Jinlong Cave in the northern section of Taihang Mountains[J]. *CARSOLOGICA SINICA*, 2023, 42(1): 149-160, 181, https://doi.org/10.11932/karst20230111, 2023.

Maloszewski, P., Stichler, W., Zuber, A., and Rank, D.: Identifying the flow systems in a karstic-fissured-porous aquifer, the Schneealpe, Austria, by modelling of environmental 18O and 3H isotopes, J Hydrol (Amst), 256, 48–59, https://doi.org/10.1016/S0022-1694(01)00526-1, 2002.

Margane, A. and Stoeckl, L.: Monitoring of spring discharge and surface water runoff in the groundwater contribution zone of Jeita Spring, Special Report No. 8 of Technical Cooperation Project “Protection of Jeita Spring”, prepared by Council for Development and Reconstruction (CDR), Lebanon, and Federal Institute for Geosciences and Natural Resources (BGR), Germany, 97 pp., 2013.

Mance, D., Radišić, M., Lenac, D., and Rubinić, J.: Hydrologicalb ehavior of karst systems identified by statistical analyses of stable isotope monitoring results, Hydrology 2022, Vol. 9, Page 82, 9, 82, https://doi.org/10.3390/HYDROLOGY9050082, 2022.

Marín, A. I., Martín Rodríguez, J. F., Barberá, J. A., Fernández-Ortega, J., Mudarra, M., Sánchez, D., and Andreo, B.: Groundwater vulnerability to pollution in karst aquifers, considering key challenges and considerations: application to the Ubrique springs in southern Spain, Hydrogeol J, 29, 379–396, https://doi.org/10.1007/S10040-020-02279-8, 2021.

Mcada, D. P., Geological Survey, U. S., Morrison, T. D., and Peck, D. L.: Sources of information and data pertaining to geohydrology in the vicinity of the Roswell Basin in parts of Chaves, Eddy, De Baca, Guadalupe, Lincoln, and Otero Counties, New Mexico, Open-File Report, https://doi.org/10.3133/OFR93144, 1993.

Miller, N., Banner, J., Feng, W., Gonzales, A., and Kozdon, R.: Hydroclimate response in Texas and Gulf of Mexico to rapid warming during the last deglacial: High-resolution speleothem proxy and monitoring evidence, Quat Sci Rev, 273, 107244, https://doi.org/10.1016/J.QUASCIREV.2021.107244, 2021.

Moerman, J. W., Cobb, K. M., Adkins, J. F., Sodemann, H., Clark, B., and Tuen, A. A.: Diurnal to interannual rainfall δ18O variations in northern Borneo driven by regional hydrology, Earth Planet Sci Lett, 369–370, 108–119, https://doi.org/10.1016/J.EPSL.2013.03.014, 2013.

Moreno, A., Sancho, C., Bartolomé, M., Oliva-Urcia, B., Delgado-Huertas, A., Estrela, M. J., Corell, D., López-Moreno, J. I., and Cacho, I.: Climate controls on rainfall isotopes and their effects on cave drip water and speleothem growth: The case of Molinos cave (Teruel, NE Spain), Clim Dyn, 43, 221–241, https://doi.org/10.1007/S00382-014-2140-6, 2014.

Mudarra Martínez, M.: Importancia relativa de la zona no saturada y zona saturada en el funcionamiento de los acuíferos carbonáticos. Caso de la alta cadena, sierra de enmedio y área de los tajos (provincia de málaga), Ph.D. thesis, Universidad de Málaga, España, 2012.

Mustafa, O., Merkel, B., and Weise, S. M.: Assessment of hydrogeochemistry and environmental isotopes in karst springs of Makook Anticline, Kurdistan Region, Iraq, Hydrology 2015, Vol. 2, Pages 48-68, 2, 48–68, https://doi.org/10.3390/HYDROLOGY2020048, 2015.

Nagra, G., Treble, P. C., Andersen, M. S., Fairchild, I. J., Coleborn, K., and Baker, A.: A post-wildfire response in cave dripwater chemistry, Hydrol Earth Syst Sci, 20, 2745–2758, https://doi.org/10.5194/HESS-20-2745-2016, 2016.

Nava-Fernandez, C., Hartland, A., Gázquez, F., Kwiecien, O., Marwan, N., Fox, B., Hellstrom, J., Pearson, A., Ward, B., French, A., Hodell, D. A., Immenhauser, A., and Breitenbach, S. F. M.: Pacific climate reflected in Waipuna Cave drip water hydrochemistry, Hydrol Earth Syst Sci, 24, 3361–3380, https://doi.org/10.5194/HESS-24-3361-2020, 2020.

Olarinoye, T., Gleeson, T., Marx, V., Seeger, S., Adinehvand, R., Allocca, V., Andreo, B., Apaéstegui, J., Apolit, C., Arfib, B., Auler, A., Barberá, J. A., Batiot-Guilhe, C., Bechtel, T., Binet, S., Bittner, D., Blatnik, M., Bolger, T., Brunet, P., Charlier, J. B., Chen, Z., Chiogna, G., Coxon, G., De Vita, P., Doummar, J., Epting, J., Fournier, M., Goldscheider, N., Gunn, J., Guo, F., Guyot, J. L., Howden, N., Huggenberger, P., Hunt, B., Jeannin, P. Y., Jiang, G., Jones, G., Jourde, H., Karmann, I., Koit, O., Kordilla, J., Labat, D., Ladouche, B., Liso, I. S., Liu, Z., Massei, N., Mazzilli, N., Mudarra, M., Parise, M., Pu, J., Ravbar, N., Sanchez, L. H., Santo, A., Sauter, M., Sivelle, V., Skoglund, R. Ø., Stevanovic, Z., Wood, C., Worthington, S., and Hartmann, A.: Global karst springs hydrograph dataset for research and management of the world's fastest-flowing groundwater, Sci Data, 7, https://doi.org/10.1038/s41597-019-0346-5, 2020.

Osácar, M. C., Sancho, C., Muñoz, A., Bartolomé, M., Moreno, A., Delgado-Huertas, A., and Cacho, I.: Tracking the oxygen isotopic signature from the rainfall to the speleothems in Ortigosa de Cameros caves (La Rioja, Spain), Estudios Geologicos, 70, https://doi.org/10.3989/EGEOL.41730.319, 2014.

Palcsu, L., Gessert, A., Túri, M., Kovács, A., Futó, I., Orsovszki, J., Puskás-Preszner, A., Temovski, M., and Koltai, G.: Long-term time series of environmental tracers reveal recharge and discharge conditions in shallow karst aquifers in Hungary and Slovakia, J Hydrol Reg Stud, 36, 100858, https://doi.org/10.1016/J.EJRH.2021.100858, 2021.

Pape, J. R., Banner, J. L., Mack, L. E., Musgrove, M. L., and Guilfoyle, A.: Controls on oxygen isotope variability in precipitation and cave drip waters, central Texas, USA, J Hydrol (Amst), 385, 203–215, https://doi.org/10.1016/J.JHYDROL.2010.02.021, 2010.

Papesch, W. and Rank, D.: Altersbestimmung (3H, 18O) an Wässern im Rahmen der Wassergüteerhebung in Tirol 1996/98: Interpretation der Meßdaten (11. Teilbericht), 1998.

Partin, J. W., Jenson, J. W., Banner, J. L., Quinn, T. M., Taylor, F. W., Sinclair, D., Hardt, B., Lander, M. A., Bell, T., Miklavic, B., Jocson, J. M. U., and Taboroši, D.: Relationship between modern rainfall variability, cave dripwater, and stalagmite geochemistry in Guam, USA, Geochemistry, Geophysics, Geosystems, 13, https://doi.org/10.1029/2011GC003930, 2012.

Pérez-Mejías, C., Moreno, A., Sancho, C., Bartolomé, M., Stoll, H., Osácar, M. C., Cacho, I., and Delgado-Huertas, A.: Transference of isotopic signal from rainfall to dripwaters and farmed calcite in Mediterranean semi-arid karst, Geochim Cosmochim Acta, 243, 66–98, https://doi.org/10.1016/J.GCA.2018.09.014, 2018.

Petitta, M., Scarascia Mugnozza, G., Barbieri, M., Bianchi Fasani, G., Esposito, C., Petitta, M., Scarascia Mugnozza, G., Barbieri, M., Bianchi Fasani, G., and Esposito, C.: Hydrodynamic and isotopic investigations for evaluating the mechanisms and amount of groundwater seepage through a rockslide dam, HyPr, 24, 3510–3520, https://doi.org/10.1002/HYP.7773, 2010.

Plagnes, V.: Structure et fonctionnement des aquifères karstiques : caractérisation par la géochimie des eaux, 1997.

Probost, G., Leis, A., Yeshegho, B., and Zojer, H.: Hydrogeologie Reisskofel-Jauken unter Berücksichtigung umweltrelevanter Kriterien, Teil 3 (KA-24E/F96). Endbericht 3. Projektjahr, unpublished report, Graz, 64pp. +Appendix pp., 1998.

Qiu, W., Yang, Y., Jiang, X., Wang, X., Wang, Y., Cai, J., Liao, Y., Feng, T., Gao, K., and Zhai, S.: Oxygen isotope variability in precipitation, dripwater, and modern calcite responding to ENSO based on 11 years' monitoring in Yuhua Cave, Southeast China, J Hydrol (Amst), 624, 129937, https://doi.org/10.1016/J.JHYDROL.2023.129937, 2023.

Reischer, M., Bichler, B., Spötl, C., Höfer-Öllinger, G., and Wyhlidal, S.: Karst hydrogeology of the Untersberg massif and its interaction with the porous aquifer in the adjacent Salzburg basin, Austrian Journal of Earth Sciences, 108, 68–81, https://doi.org/10.17738/ajes.2015.0014, 2015.

Ren, K., Zeng, J., Liang, J., Yuan, D., Jiao, Y., Peng, C., and Pan, X.: Impacts of acid mine drainage on karst aquifers: Evidence from hydrogeochemistry, stable sulfur and oxygen isotopes, Science of The Total Environment, 761, 143223, https://doi.org/10.1016/J.SCITOTENV.2020.143223, 2021.

Ren, K., Pan, X., Yuan, D., Zeng, J., Liang, J., and Peng, C.: Nitrate sources and nitrogen dynamics in a karst aquifer with mixed nitrogen inputs (Southwest China): Revealed by multiple stable isotopic and hydro-chemical proxies, Water Res, 210, 118000, https://doi.org/10.1016/J.WATRES.2021.118000, 2022.

Ridley, H. E., Baldini, J. U. L., Prufer, K. M., Walczak, I. W., and Breitenbach, S. F. M.: High-resolution monitoring of Yok Balum Cave, Belize: An investigation of seasonal ventilation regimes and the atmospheric and drip-flow response to a local earthquake, Journal of Cave and Karst Studies, 77, 183–199, https://doi.org/10.4311/2014ES0117, 2015.

Riechelmann, D. F. C., Schröder-Ritzrau, A., Scholz, D., Fohlmeister, J., Spötl, C., Richter, D. K., and Mangini, A.: Monitoring Bunker Cave (NW Germany): A prerequisite to interpret geochemical proxy data of speleothems from this site, J Hydrol (Amst), 409, 682–695, https://doi.org/10.1016/J.JHYDROL.2011.08.068, 2011.

Riechelmann, D. F. C., Deininger, M., Scholz, D., Riechelmann, S., Schröder-Ritzrau, A., Spötl, C., Richter, D. K., Mangini, A., and Immenhauser, A.: Disequilibrium carbon and oxygen isotope fractionation in recent cave calcite: Comparison of cave precipitates and model data, Geochim Cosmochim Acta, 103, 232–244, https://doi.org/10.1016/J.GCA.2012.11.002, 2013.

Riechelmann, S., Schröder-Ritzrau, A., Spötl, C., Riechelmann, D. F. C., Richter, D. K., Mangini, A., Frank, N., Breitenbach, S. F. M., and Immenhauser, A.: Sensitivity of Bunker Cave to climatic forcings highlighted through multi-annual monitoring of rain-, soil-, and dripwaters, Chem Geol, 449, 194–205, https://doi.org/10.1016/J.CHEMGEO.2016.12.015, 2017.

Ronchetti, F., Deiana, M., Lugli, S., Sabattini, M., Critelli, V., Aguzzoli, A., and Mussi, M.: Water isotope analyses and flow measurements for understanding the stream and meteoric recharge contributions to the Poiano evaporite karst spring in the North Apennines, Italy, Hydrogeol J, 31, 601–619, https://doi.org/10.1007/S10040-023-02604-X/TABLES/5, 2023.

Schmidt, S.: Hydrogeological characterisation of karst aquifers in semi-arid environments at the catchment scale – Example of the Western Lower Jordan Valley, PhD thesis, Georg-August-Universität Göttingen, Göttingen, Germany, 2014.

Smith, A. C., Wynn, P. M., Barker, P. A., Leng, M. J., Noble, S. R., and Stott, A.: Cave monitoring and the potential for palaeoclimate reconstruction from Cueva de Asiul, Cantabria (N. Spain), International Journal of Speleology, 45: 1-9. http://dx.doi.org/10.5038/1827-806X.45.1.1928, 2015.

Spötl, C., Fairchild, I. J., and Tooth, A. F.: Cave air control on drip water geochemistry, Obir Caves (Austria): Implications for speleothem deposition in dynamically ventilated caves, Geochim Cosmochim Acta, 69, 2451–2468, https://doi.org/10.1016/J.GCA.2004.12.009, 2005.

Stroj, A., Briški, M., and Oštrić, M.: Study of groundwater flow properties in a karst system by coupled analysis of diverse environmental tracers and discharge dynamics, Water 2020, Vol. 12, Page 2442, 12, 2442, https://doi.org/10.3390/W12092442, 2020.

Surić, M., Lončarić, R., Lončar, N., Buzjak, N., Bajo, P., and Drysdale, R. N.: Isotopic characterization of cave environments at varying altitudes on the eastern Adriatic coast (Croatia) – Implications for future speleothem-based studies, J Hydrol (Amst), 545, 367–380, https://doi.org/10.1016/J.JHYDROL.2016.12.051, 2017.

Surić, M., Lončarić, R., Bočić, N., Lončar, N., and Buzjak, N.: Monitoring of selected caves as a prerequisite for the speleothem-based reconstruction of the Quaternary environment in Croatia, Quaternary International, 494, 263–274, https://doi.org/10.1016/J.QUAINT.2017.06.042, 2018.

Tadros, C. V., Treble, P. C., Baker, A., Fairchild, I., Hankin, S., Roach, R., Markowska, M., and McDonald, J.: ENSO-cave drip water hydrochemical relationship: A 7-year dataset from south-eastern Australia, Hydrol Earth Syst Sci, 20, 4625–4640, https://doi.org/10.5194/HESS-20-4625-2016, 2016.

Tadros, C. V., Markowska, M., Treble, P. C., Baker, A., Frisia, S., Adler, L., and Drysdale, R. N.: Recharge variability in Australia's southeast alpine region derived from cave monitoring and modern stalagmite δ18O records, Quat Sci Rev, 295, 107742, https://doi.org/10.1016/J.QUASCIREV.2022.107742, 2022.

Tian, L., Gao, Y., Yang, G., Schwartz, B., Cai, B., Ray, C., Li, Y., and Wu, H.: Isotopic tracers of sources of water for springs from the Edwards Aquifer, Central Texas, USA, Hydrology Research, 52, 787–803, https://doi.org/10.2166/NH.2021.011, 2021a.

Tian, Y., Zhang, H., Zhang, R., Zhang, F., Liang, Z., Cai, Y., and Cheng, H.: Seasonal and Inter-Annual Variations of Stable Isotopic Characteristics of Rainfall and Cave Water in Shennong Cave, Southeast China, and Its Paleoclimatic Implication, Front Earth Sci (Lausanne), 9, 794762, https://doi.org/10.3389/FEART.2021.794762, 2021b.

Treble, P. C., Bradley, C., Wood, A., Baker, A., Jex, C. N., Fairchild, I. J., Gagan, M. K., Cowley, J., and Azcurra, C.: An isotopic and modelling study of flow paths and storage in Quaternary calcarenite, SW Australia: implications for speleothem paleoclimate records, Quat Sci Rev, 64, 90–103, https://doi.org/10.1016/J.QUASCIREV.2012.12.015, 2013.

Treble, P. C., Fairchild, I. J., Griffiths, A., Baker, A., Meredith, K. T., Wood, A., and McGuire, E.: Impacts of cave air ventilation and in-cave prior calcite precipitation on Golgotha Cave drip water chemistry, southwest Australia, Quat Sci Rev, 127, 61–72, https://doi.org/10.1016/J.QUASCIREV.2015.06.001, 2015.

Treble, P. C., Baker, A., Abram, N. J., Hellstrom, J. C., Crawford, J., Gagan, M. K., Borsato, A., Griffiths, A. D., Bajo, P., Markowska, M., Priestley, S. C., Hankin, S., and Paterson, D.: Ubiquitous karst hydrological control on speleothem oxygen isotope variability in a global study, Communications Earth & Environment 2022 3:1, 3, 1–10, https://doi.org/10.1038/s43247-022-00347-3, 2022.

Turin, H. J., Plummer, M. A., and Phillips, F. M.: Tritium, Chlorine-36, and water isotopologue profiles from Lechuguilla Cave and Carlsbad Cavern, New Mexico, USA, Applied Geochemistry, 138, 105212, https://doi.org/10.1016/J.APGEOCHEM.2022.105212, 2022.

USGS Water Data for the Nation: https://waterdata.usgs.gov/nwis, last access: 14 April 2025.

Vieten, R., Warken, S., Winter, A., Schröder-Ritzrau, A., Scholz, D., and Spötl, C.: Hurricane Impact on Seepage Water in Larga Cave, Puerto Rico, J Geophys Res Biogeosci, 123, 879–888, https://doi.org/10.1002/2017JG004218, 2018a.

Vieten, R., Warken, S., Winter, A., Scholz, D., Miller, T., Spötl, C., and Schröder-Ritzrau, A.: Monitoring of Cueva Larga, Puerto Rico—A First Step to Decode Speleothem Climate Records, 319–331, https://doi.org/10.1007/978-3-319-51070-5_36, 2018b.

Wang, Q., Wang, Y., Zhao, K., Chen, S., Liu, D., Zhang, Z., Huang, W., Yang, S., and Liang, Y.: The transfer of oxygen isotopic signals from precipitation to drip water and modern on the seasonal time scale in Yongxing Cave, central China, Environ Earth Sci, 77, 474, https://doi.org/10.1007/S12665-018-7607-Z, 2018.

Wang, Z., Guo, X., Kuang, Y., Chen, Q., Luo, M., and Zhou, H.: Recharge sources and hydrogeochemical evolution of groundwater in a heterogeneous karst water system in Hubei Province, Central China, Applied Geochemistry, 136, 105165, https://doi.org/10.1016/J.APGEOCHEM.2021.105165, 2022.

Warken, S. F., Fohlmeister, J., Schröder-Ritzrau, A., Constantin, S., Spötl, C., Gerdes, A., Esper, J., Frank, N., Arps, J., Terente, M., Riechelmann, D. F. C., Mangini, A., and Scholz, D.: Reconstruction of late Holocene autumn/winter precipitation variability in SW Romania from a high-resolution speleothem trace element record, Earth Planet Sci Lett, 499, 122–133, https://doi.org/10.1016/J.EPSL.2018.07.027, 2018.

Warken, S. F., Kuchalski, L., Schröder-Ritzrau, A., Vieten, R., Schmidt, M., Höpker, S. N., Hartland, A., Spötl, C., Scholz, D., and Frank, N.: The impact of seasonal and event-based infiltration on transition metals (Cu, Ni, Co) in tropical cave drip water, Rapid Communications in Mass Spectrometry, 36, e9278, https://doi.org/10.1002/RCM.9278, 2022.

Wieselthaler, F.: Abflusskomponentenanalyse bei einer Karstquelle auf der Basis von Ereignisuntersuchungen (Wasseralmquelle, Schneealpe), Diplomarbeit, Universität Wien, Vienna, Austria, 2006.

Williams, P. W. and Fowler, A.: Relationship between oxygen isotopes in rainfall, cave percolation waters and speleothem calcite at Waitomo, New Zealand, 2002.

Yin, J. J., Tang, W., Wu, X., Pu, J., Zhu, X., Wang, Z., Lan, G., and Yang, H.: Individual event, seasonal and interannual variations in δ18O values of drip water in Maomaotou Big Cave, Guilin, South China, and their implications for palaeoclimatic reconstructions, Boreas, 49, 769–782, https://doi.org/10.1111/BOR.12454, 2020.

Yu, S., Chae, G., Oh, J., Kim, S. H., Kim, D. Il, and Yun, S. T.: Hydrochemical and isotopic difference of spring water depending on flow type in a stratigraphically complex karst area of South Korea. Front. Earth Sci. 9:712865, https://doi.org/10.3389/FEART.2021.712865, 2021.

Zengin, E.: Isotopic study of the waters from the Sulphur Springs catchment, Tampa, Florida, Master thesis, University of South Florida, USA, 2022.

Zhao, J., Tan, L., Li, D., Pérez-Mejías, C., Dong, X., Wang, J., Zhang, H., and Cheng, H.: The seasonally altered atmosphere moisture circulations with rainfall and rainfall isotopes in Southwest China, Front Earth Sci (Lausanne), 10, 795857, https://doi.org/10.3389/FEART.2022.795857, 2022.

Zhao, M., Hu, Y., Zeng, C., Liu, Z., Yang, R., and Chen, B.: Effects of land cover on variations in stable hydrogen and oxygen isotopes in karst groundwater: A comparative study of three karst catchments in Guizhou Province, Southwest China, J Hydrol (Amst), 565, 374–385, https://doi.org/10.1016/J.JHYDROL.2018.08.037, 2018.